

1  
2  
3  
4  
5  
6  
7  
8  
9  
10  
11  
12  
13  
14  
15  
16  
17  
18  
19  
20  
21  
22  
23

**Preprint of “The Largest Mountain Belt of the Last Billion Years: The East African Orogen, its tectono-topographic evolution and global significance.”**

by

**Collins, A.S.<sup>1\*</sup>, Blades, M.L.<sup>1</sup>, Hasterok, D.<sup>1</sup>, Cameron, F.<sup>1</sup>, Razakamanana, T.<sup>2</sup>, Merdith, A. S.<sup>1</sup>, Foden, J.D<sup>1</sup>, Clark, C.<sup>3</sup>**

<sup>1</sup>*Tectonics and Earth Systems (TES), Department of Earth Sciences, Adelaide University, Adelaide, SA 5005, Australia. \* = alan.collins@adelaide.edu.au*

<sup>2</sup>Département des Sciences de la Terre, Université de Toliara, Toliara, Madagascar

<sup>5</sup>School of Earth and Planetary Sciences, Curtin University, Perth, Australia

This paper is a non-peer reviewed preprint submitted to EarthArXiv

It is submitted for publication consideration In: Harley, S. (ed) *In the Footsteps of Hutton A celebration of the tercentenary of the Birth of James Hutton. Geological Society, London, Special Publication.*

24 The Largest Mountain Belt of the Last Billion Years: The East  
25 African Orogen, its tectono-topographic evolution and global  
26 significance.

27 Collins, A.S.<sup>1</sup>, Blades, M.L.<sup>1</sup>, Hasterok, D.<sup>1</sup>, Cameron, F.<sup>1</sup>, Razakamanana, T.<sup>2</sup>, Merdith, A. S.<sup>1</sup>,  
28 Foden, J.D<sup>1</sup>, Clark, C.<sup>3</sup>

29  
30 <sup>1</sup>*Tectonics and Earth Systems (TES), Department of Earth Sciences, Adelaide University, Adelaide,*  
31 *SA 5005, Australia.*

32 <sup>2</sup>Département des Sciences de la Terre, Université de Toliara, Toliara, Madagascar

33 <sup>5</sup>School of Earth and Planetary Sciences, Curtin University, Perth, Australia

34  
35 **ABSTRACT**

36 Hutton's Principle of Uniformitarianism suggests that the present is the key to the past,  
37 and in the present, Earth's topography is dominated by the Himalaya. The geological record  
38 clearly preserves past mountain ranges, but few have purported to have the effect on Earth's  
39 surface systems (such as the atmosphere, hydrosphere, biosphere and ocean chemistry) that the  
40 Himalaya does today. The Neoproterozoic East African Orogen is an exception. Not only is it the  
41 scale of the modern Himalaya, but it affected ocean chemistry in a similar manner to the  
42 Himalaya. Here we posit that the East African Orogen is the only other Himalayan-scale mountain  
43 range, and the only orogen that contends with the Himalaya as the largest mountain range of the  
44 last billion years.

45 In this manuscript we review and reconstruct the orogen. We then use existing  
46 metamorphic data triaged to exclude subduction-zone metamorphism, to estimate the  
47 elevation-time evolution of the orogen. We demonstrate that the available metamorphic record  
48 supports our assertion that the East African Orogen is amongst the largest orogens in the  
49 geological record. We also integrate spatially-located metamorphic data with a full-plate tectonic  
50 reconstruction of the evolving orogen to show how different plate interactions created the  
51 evolving topography.

52

53 **INTRODUCTION**

54 Mountain belts transport material from the deep Earth to the reactive crucible of the planet's  
55 surface, where it interacts with the atmosphere and hydrosphere and biosphere. This element-  
56 transfer role of mountains controls such fundamental uniformitarian Earth processes as the  
57 supply and extraction of CO<sub>2</sub> to and from the atmosphere, for example chemical weathering of  
58 large mountain ranges can push the planet towards icehouse conditions (Godderis et al., 2017).  
59 Weathering of mountain ranges also supplies nutrients that facilitate biological productivity and  
60 help drive evolution (Cox et al., 2016b; Yang et al., 2020). A major step in understanding how our  
61 planet evolved and developed as a system is to understand the history, location and evolution of  
62 past mountain ranges (e.g. Merdith et al., Submitted).

63

64 We can track the fingerprints of past mountain ranges by variations in the products of extremely  
65 long half-life radioactive decay systems into the oceans. The most useful of these is <sup>87</sup>Sr, which  
66 forms by radioactive decay of <sup>87</sup>Rb that is relatively common in the lithosphere and has a suitably  
67 long half-life of 4.92×10<sup>10</sup> years. Strontium is soluble in water and has a residence time in the  
68 oceans on the order of millions of years (Veizer et al., 1999; Vollstaedt et al., 2014), meaning that  
69 it is well mixed in the oceans. It also readily precipitates with carbonates. These features mean  
70 that strontium isotopes form an effective proxy for the erosion of old rocks—rocks that get  
71 brought to the surface and eroded in mountain ranges. Therefore, the strontium isotope curve  
72 for carbonates through the last billion years contains within it the globally homogenized orogenic  
73 record through that time. For example, the growth of the Himalaya over the last 50 Ma is  
74 reflected in a sharp rise in radiogenic strontium (Derry and France-Lanord, 1996). The only other  
75 instance in the last billion years with a similar rise was between ca. 850–500 Ma, particularly  
76 focused between ca. 660–500 Ma (Shields, 2007; Cox et al., 2016a; Chen et al., 2022). This period  
77 coincides with the formation of the Gondwana-forming orogens (Collins and Pisarevsky, 2005;  
78 Cawood and Buchan, 2007; Schmitt et al., 2018)(Fig. 1), of which the East African Orogen is the  
79 largest in both spatial footprint and elevation (Fritz et al., 2013; Clark et al., 2015)(Figs. 1, 2).

80

81 Geographic reconstructions that divide the earth into land and sea have been a research focus  
82 since the development of the continental drift hypothesis (Wegener, 1912). Palaeomagnetic-  
83 based continental drift-like models that focus on continent distributions (Dalziel, 1997; Li et al.,  
84 2008) have evolved into full-plate tectonic reconstructions that use the wealth of palaeotectonic  
85 information held in global rock systems to attempt to reconstruct plate tectonics in deep time  
86 (Domeier and Torsvik, 2014; Domeier, 2016; Merdith et al., 2017a; Merdith et al., 2021; Li et al.,  
87 2023; Cao et al., 2024). Restoring the horizontal motion of Earth's lithosphere is not enough,  
88 though, to accurately model the importance of the geosphere on Earth surface systems. We also  
89 need to understand the geographic expression and distribution of Earth's surface topography  
90 (and bathymetry). This has been attempted in the Phanerozoic by looking at preserved rocks and  
91 attributing an elevation to that part of the world at the time of rock formation. For example, the  
92 presence of preserved deep marine, shallow marine and terrestrial sedimentary rocks indicates  
93 past flooded continents and coastal elevations. The presence of mountains is usually invoked  
94 from the preservation of metamorphic rocks on the surface, exhumed by erosion of the orogenic  
95 topography (e.g. Scotese, 2021). More quantitative approaches using the geochemistry of  
96 igneous rocks that formed in specific tectonic settings (like volcanic arcs, or mountain belts) have  
97 been developed that provide estimates of crustal thickness at the time of crystallisation, and  
98 therefore information about past topography (Tang et al., 2021; Zhu et al., 2022; Zhou et al.,  
99 2025). These approaches require magmatism, and many of the largest mountain ranges in the  
100 world have limited magmatism during the times at which they have maximum elevation (e.g. the  
101 Himalaya today). Here, we take a complementary approach to look at past-orogenic elevations,  
102 by reviewing the pressure-time history preserved in metamorphic rocks and use these to  
103 estimate past-orogenic elevation (Collins et al., 2022b).

104

105 In this manuscript, we first review the extent and nature of the preserved rocks within the East  
106 African Orogen (Fig. 1), as one of the largest orogens known in the geological record, place them  
107 within a modern full-plate tectonic framework, and qualitatively discuss the spatial and temporal  
108 evolution of major topography. We aim that our method forms a focus for future investigations

109 into quantitative estimates of elevation to understand how orogenic evolution modulates Earth  
110 system.

111

## 112 **THE CONCEPT OF THE EAST AFRICAN OROGEN**

113 The East African Orogen (EAO; Figs. 1, 2) was defined by Stern (1994). Here we restrict it to the  
114 regions where rocks crop out or are found in the subsurface that were formed and/or deformed  
115 in a mountain range that ran through the centre of Palaeozoic Gondwana (Fig. 1). The orogen  
116 forms a broad band from northernmost Gondwana—Egypt and the Middle East, and now  
117 dispersed terranes that reconstruct to this region—through eastern Africa and Madagascar (Figs.  
118 1, 2). South of Madagascar, in reconstructed Gondwana, the orogen bifurcated into two branches  
119 (Fig. 2). A western branch joins with the Zambezi Belt of Zambia and Zimbabwe and then to the  
120 Lufilian Arc and the central Damara Belt (Goscombe et al., 2020)(Figs. 1, 2). An eastern branch  
121 passes through southernmost India, Sri Lanka and into the Lützow-Holm Bay area of eastern  
122 Antarctica (Plavsa et al., 2015) ('Lut' in Fig. 2). Here we will focus on the region north of this  
123 bifurcation, where the EAO is clearly the result of ocean closure and subsequent continent-  
124 continent collision between Neoproterozoic India and the Neoproterozoic African continents—  
125 the southern Congo-Tanzania-Bangweulu continent and the Saharan metacraton (Figs. 1, 2). The  
126 boundary between these two continents is the Central African Fold Belt (otherwise known as the  
127 Oubanguides belt)(Figs. 1,2), which consists of a series of thrust sheets, known as the Yaoundé-  
128 Yangana nappes (Toteu et al., 2022)("Y-Y" in Fig. 2) transported south over the Congo-Tanzania-  
129 Bangweulu Block. The belt marks a site of ocean closure that separates a Neoproterozoic arc  
130 terrane (Poli- Mayo Kebbi arc) from the Congo-Tanzania-Bangweulu continent and can be traced  
131 west into the Sergipano belt of NE Brazil (Neves et al., 2006)(Fig. 1).

132

133 The EAO divided Gondwana into an eastern part, whose major components now form South  
134 America and Africa, and a western part, whose now dispersed successors form Australia, East  
135 Antarctica, India and much of East Asia (Fig. 1). In our discussion here we refer to directions in a  
136 reconstructed Gondwana reference frame with Africa oriented as present day. The significance  
137 of the EAO was increased when McWilliams (1981) supported early speculation that plate

138 tectonics operated in the Precambrian (Burke et al., 1976) and interpreted the palaeomagnetic  
139 data of the times to reflect the existence of two large, separately travelling, continents that  
140 collided to form Gondwana in the late Proterozoic. Stern (1994), delineated and named the EAO  
141 and suggested that this was the site of collision between these east and west Neoproterozoic  
142 Gondwana continents. This led to a hunt for the suture of the newly named Mozambique Ocean  
143 that was hypothesized to have separated these continents (Shackleton, 1996).

144  
145 In 1997, Ian Dalziel began the push to map the deep time geography of the planet by publishing  
146 a major continental-drift style reconstruction for the Neoproterozoic (Dalziel, 1997) that  
147 attempted to combine known geology with the palaeomagnetic record. This model coincided  
148 with Joe Meert and Rob Van der Voo (1997) pointing out that the developing geochronological  
149 record for the formation of Gondwana appeared to show three main periods of orogenesis. The  
150 earliest orogeny, between 800–650 Ma, was correlated with the East African Orogeny and was  
151 located mainly in East Africa. A second orogeny was interpreted as representing the  
152 amalgamation of the South American part of Gondwana between 600–530 Ma. A third, eastern  
153 Gondwanan orogeny, was suggested to have occurred at ca. 550 Ma. They named this the Kuunga  
154 Orogeny and suggested that it involved the final amalgamation of Gondwana (Meert and Van der  
155 Voo, 1997).

156  
157 At about this time, several researchers realized that the vast region of the EAO preserved  
158 evidence of considerable orogenic complexity, like that of Phanerozoic orogens. Kröner et al.  
159 (2000) and Collins and Windley (2002) suggested that a major piece of pre-Neoproterozoic  
160 continental crust lay within the East African Orogen. This palaeocontinent was subsequently  
161 named 'Azania' (Collins and Pisarevsky, 2005) (Figs. 1, 2). It was proposed that Azania collided  
162 with the Congo-Tanzania-Bangweulu continent at ca. 650 Ma and that this collision was the event  
163 responsible for the East African Orogeny. Neoproterozoic India was hypothesized to have later  
164 collided with the then combined Azania/Congo-Tanzania-Bangweulu continent at ca. 550 Ma  
165 forming a Malagasy Orogeny (Collins and Pisarevsky, 2005). Meanwhile, Johnson and  
166 Woldehaimanot (2003) published a key review of the northern EAO in the Arabian Nubian Shield

167 (Fig. 2). They demonstrated that this vast area, which incorporated all of Arabia and much of NE  
168 Africa, consisted of a series of different-aged terranes that amalgamated at different times in a  
169 similar, but better resolved, manner that Collins and coworkers were proposing in the southern  
170 EAO. Johnson et al. (2011) and Fritz et al. (2013) published major reviews of the northern and  
171 southern parts of the EAO.

172  
173 The last 20 years has seen the identification of further pre-Neoproterozoic crust within the EAO  
174 that has extended the number and complexity of continental terranes within the orogen (Be'eri-  
175 Shlevin et al., 2009; Be'eri-Shlevin et al., 2012; Boger et al., 2014a; Eyal et al., 2014; Boger et al.,  
176 2015; Clark et al., 2020). Both margins of the EAO have been significantly revised and extended.  
177 Here we suggest that the eastern margin be extended to include the basement of Oman,  
178 Seychelles, Pakistan and NW India (Alessio et al., 2018; Blades et al., 2020; Collins et al., 2021b;  
179 de Wall et al., 2022) (Figs. 1, 2). In these regions, juvenile Tonian (1000 to ca. 720 Ma, this and all  
180 stratigraphic ages taken from Cohen et al., 2025) crust forms the basement, but in contrast to  
181 the western EAO, orogenesis ended in the late Tonian or earliest Cryogenian (ca. 720–635 Ma).

182  
183 The original definition of the western margin of the EAO as the boundary with a “Saharan  
184 Metacraton” (Abdelsalam et al., 2002) is also far from clear and needs significant revision,  
185 especially with the identification of Ediacaran (ca. 635–539 Ma) juvenile terranes in northern  
186 Chad in the centre of the erstwhile “Saharan Metacraton” (Şengör et al., 2020; Shellnutt et al.,  
187 2026). In Chad, a pre-Neoproterozoic terrane has been identified and named the Poli-Mayo  
188 Kebbi-Lake Fitri Terrane (PMKF)(Fig. 1). To date there are no pre-Neoproterozoic rocks known  
189 from this region and it appears to be a juvenile Tonian terrane (Shellnutt et al., 2026). Southeast  
190 of the PMKF lies the Adamawa-Yadé-Guéra-Ouaddaï (AYGO) Terrane (Fig. 1)(Shellnutt et al.,  
191 2026). This contains gneisses with protoliths that date back to the Stenian (1000–1200  
192 Ma)(Blades et al., 2021a), with detrital and inherited zircons that reach back to the Archaean  
193 (Djerossem et al., 2020; Blades et al., 2021a). These contrast with other parts of the Saharan  
194 basement, for example Gebel Uweinat in SW Egypt, that preserve Archaean rocks that have  
195 largely missed later orogenesis (Zhang et al., 2019)(Fig. 1). A boundary between pre-

196 Neoproterozoic and Tonian crust marks the edge of the EAO as shown in figures 1 and 2. Juvenile  
197 Neoproterozoic terranes then characterize the western parts of the EAO (west of Afif-Abas and  
198 Azania, Fig. 2). The 800–650 Ma East African Orogeny of Meert and Van der Voo (1997) affected  
199 these regions, but the later Malagasy Orogeny (correlated with the Angudan Orogeny in Arabia,  
200 Collins and Pisarevsky, 2005) largely, did not (with only local shear zones being active at this  
201 time).

202  
203 The origin and tectono-geographic location of the EAO have been revised considerably. The  
204 original suggestion, that the orogen preserved a Tonian continental rift sequence that  
205 represented the break-up of Rodinia (Stern, 1994), is no longer tenable, as extensive Stenian crust  
206 has been identified along the west margin of the EAO (de Wit and Linol, 2015; Blades et al.,  
207 2021b) and within the EAO in Madagascar, Sinai and East Antarctica (Eyal et al., 2014; Tucker et  
208 al., 2014; Jacobs et al., 2015; Elburg et al., 2016; Archibald et al., 2018). In addition, the age of  
209 800 Ma for the beginning of the East African Orogeny (Meert and Van der Voo, 1997) is  
210 challenged by extensive 850–750 Ma magmatism in central Madagascar (Handke et al., 1997;  
211 Archibald et al., 2016; Archibald et al., 2017), pre-800 Ma magmatism in Ethiopia (Blades et al.,  
212 2015; Bowden et al., 2020), Arabia (Whitehouse et al., 2016; Alessio et al., 2018), NW India and  
213 SE Pakistan (Pandit et al., 2003; Shakoor et al., 2019), South India (Plavsa et al., 2015) and Sri  
214 Lanka (Kröner and Jaeckel, 1994). A window into the basement in NE Oman demonstrates the  
215 presence of high-grade metamorphism and deformation at ca. 820 Ma (Alessio et al., 2018) that  
216 links with pre-760 Ma tectonothermal activity recorded in the Pakistan and India basement west  
217 of the Western Margin Fault of the Aravalli-Delhi Fold Belt India (Deb et al., 2001; de Wall et al.,  
218 2022), showing that pre-800 Ma orogenesis is not limited to magmatism. We suggest that the  
219 orogen should now be thought to represent over 500 million years of punctuated subduction-  
220 accretion. This new paradigm means that the orogen does not represent a Wilson-like, internal  
221 ocean (Nance et al., 1988), opening and closing in approximately the same position. Instead, it  
222 seems clear that the orogen lay in a tectono-geographic position like that of the modern Pacific-  
223 rim, where subduction of an external ocean over hundreds of millions of years resulted in a  
224 punctuated record of accretion, extension, arc magmatism and collision (Merdith et al., 2017b;

225 Şengör et al., 2020; Collins et al., 2021b; Merdith et al., 2021). This process is similar to the  
226 Proterozoic to Mesozoic history of the Central Asian Orogenic Belt (Kröner et al., 2014; Xiao et  
227 al., 2020) and the Phanerozoic history of the Tasmanides of Australia and the broader Terra  
228 Australis Orogen (Cawood, 2005; Glen and Meffre, 2009; Rosenbaum, 2018).

229  
230 In the next section, we summarize the Stenian to Cambrian (ca. 1100–520 Ma) history of the now  
231 dispersed parts of the EAO before we discuss the tectonic geography of their amalgamation and  
232 evolution of the resulting mountain range(s).

233

## 234 **THE FAR NORTHERN EAST AFRICAN OROGEN**

### 235 ***Displaced terranes in Greece, Türkiye and Iran***

236

237 Tectonic windows into Neoproterozoic to early Palaeozoic crust occur as discontinuous  
238 exposures throughout the central crystalline basement of Europe and from the Alps to Türkiye,  
239 Syria and Iran in the Alpine–Mediterranean mountain belt (von Raumer et al., 2003). The  
240 orogenesis preserved in these locations are variously attributed to the Cadomian or East African  
241 orogen events (often just termed ‘Pan-African’). The precise original location of these now exotic  
242 terranes are hard to define. However, the limited Mesozoic ocean crust development in the  
243 western Mediterranean and (near?)continuity of the Apulia promontory with both northern  
244 Gondwana and northern Europe means that the Aegean and eastern Mediterranean terranes are  
245 restricted to originate close to the Egyptian margin of north Gondwana (Stampfli, 2005; Torsvik  
246 and Cocks, 2013)(Fig. 2), close to where the East African Orogen met the circum-Gondwana  
247 Ocean (which at this part of geological time and at this location is named the Tornquist Sea).

248

249 The terranes most pertinent here are the Greek Pelagonian Zone, the Turkish Tauride Terranes  
250 (the Menderes Massif and the Bitlis Massif), as well as the dismembered terranes of the  
251 Sanandaj–Sirjan Zone of Iran as these formed the far northern extensions of the EAO (Fig. 2). The  
252 Pelagonian Zone of Greece contains the relatively small Florina Terrane, which preserves  
253 orthogneisses dated as crystallizing between ca. 730–690 Ma (Anders et al., 2006). Crystallization

254 ages of this antiquity have not been recorded from the Menderes Massif that is found along  
255 tectonic strike in west Türkiye. Here, an old kernel of Neoproterozoic clastic metasedimentary  
256 rocks are intruded by 570–520 Ma granites (Gessner et al., 2004; Koralay et al., 2004) with rare  
257 metabasites that preserve Cambrian eclogite metamorphic assemblages (Candan et al., 2016). A  
258 similar Proterozoic clastic sequence is preserved in the Bitlis Massif of SE Türkiye, here also,  
259 purported subduction-related magmatic rocks intrude the sequence at ca. 550–530 Ma  
260 (Ustaomer et al., 2009). The Iranian Sanandaj-Sirjan Zone, contains a series of inliers of  
261 Neoproterozoic–Cambrian metasedimentary rocks and granitoids decorating the Cenozoic  
262 suture (Jamshidi-Badr et al., 2013; Fergusson et al., 2016; Honarmand et al., 2018). Further east  
263 in Iran, the ‘Central and East Iranian Microcontinent’ (CEIM) consists of three blocks (the Lut,  
264 Tabas and Yazd) separated by tectonic belts. In one of these belts, 575–525 Ma granitoids that  
265 have been attributed to an Andean-like volcanic arc, suggest that this region shares a similar  
266 Ediacaran–Cambrian tectonic setting to the other basement terranes in Türkiye and Iran  
267 (Ramezani and Tucker, 2003; Rossetti et al., 2015). The continental volcanic-arc tectonic setting  
268 of these has been questioned by Zoleikhaei et al. (2025), who argued that the detrital zircon and  
269 apatite record in Ediacaran to Palaeozoic sandstones, is better explained by a rift setting at this  
270 time with no arc-like edifice.

271  
272 Both Ediacaran–Cambrian intrusions in the Sanandaj–Sirjan Zone and in the Menderes Massif  
273 preserve inherited zircon that stretches back to ca. 3.6 Ga and hafnium isotopes on younger  
274 grains that suggest ancient continent was a component of the source of these rocks (Nutman et  
275 al., 2014). Whether this ancient source was crystalline basement beneath those regions, or  
276 detritus then preserved in Proterozoic metasedimentary rocks is unclear.

277  
278 **THE NORTHWESTERN EAST AFRICAN OROGEN: THE ARABIAN NUBIAN SHIELD (ANS)**  
279 ***Egypt, Sudan, Saudi Arabia, Eritrea, central and north Ethiopia, Yemen, northern Somalia***

280  
281 The ANS (Fig. 2) is dominated by low grade volcano-sedimentary sequences and associated  
282 plutonic and ophiolitic remnants. These are reconstructed into a complex mix of terranes

283 representing accreted arcs that record subduction polarity reversals that are reviewed and  
284 summarised in a number of papers (Johnson et al., 2011; Robinson et al., 2014; Kashghari et al.,  
285 2025).

286  
287 Pre-Stenian (> 1200 Ma) crust in the ANS forms two broad belts. One extends from the  
288 Palaeoproterozoic Khida region of Saudi Arabia (which also underlies much of the Siham-Khida  
289 Terrane—previously part of the Afif Terrane—to the north; Stoeser and Frost, 2006)(“SK” in Fig.  
290 2) to the Abas Terrane of Yemen (Yeshanew et al., 2015; Whitehouse et al., 2023)(“Ab” in Fig. 2).  
291 The Neoproterozoic Al-Bayda Terrane separates the Abas Terrane from the Palaeoproterozoic–  
292 Archaean Al-Mafid Terrane of southern Yemen (“Ab” and “AMa” respectively in Fig. 2). The Al-  
293 Mafid Terrane is traced south across to the Somaliland escarpment (Sassi et al., 1993), and  
294 further south through eastern Ethiopia (Kröner and Sassi, 1996) to southern Somalia (Küster et  
295 al., 1990), central Madagascar (Kröner et al., 2000) and into southern India (Collins and Windley,  
296 2002; Collins et al., 2007; Plavsa et al., 2014)(Fig. 2). Collins and Pisarevsky (2005) named this pre-  
297 Stenian microcontinent ‘Azania’ after the ancient Greek name for the east African Coast (Schoff,  
298 1912).

299  
300 The next oldest terrane in the ANS is the late Mesoproterozoic Sa’al Metamorphic Complex  
301 (1.03–1.02 Ga) in Sinai, marking the initiation of magmatism in the northern-most Arabian  
302 Nubian Shield (Be’eri-Shlevin et al., 2012; Eyal et al., 2014)(Fig. 2). The original location of this  
303 Stenian terrane, is uncertain, due to it being surrounded by younger terranes, but coeval  
304 subduction-magmatism occurred within the Saharan basement (Blades et al., 2021b) and the  
305 Sinai terrane may form a rifted part of this continent.

306  
307 The Tonian to Cryogenian history of the ANS is marked by formation of oceanic volcanic arcs and  
308 arcs built on Azanian (or Afif-Abas) crust that amalgamated to form a larger intra-Mozambique  
309 Ocean terrane separate from both Neoproterozoic India and African Gondwanan continents. A  
310 number of terranes in the ANS are correlated as equivalents, separated by the opening of the  
311 Red Sea, from south to north, these are the Asir (a composite of the Bidah, An Nimas, Al Qarah-

312 Malahah and Tathlith terranes of Kashghari et al., 2025) and Tokar/Barka terranes, the Haya and  
313 Jiddah terranes, the Hijaz and Gabgaba/Gebeit terranes, and the Eastern Desert and Midyan  
314 terranes (Johnson et al., 2011)(Fig. 2). It is unclear whether the combined Asir-Tokar/Barka  
315 terrane and Haya-Jiddah terranes were ever on separate plates as, in Saudi Arabia, no clear  
316 suture is seen between them (Kashghari et al., 2025). In SE Sudan and Eritrea, the Tokar-Barka  
317 terrane (Fig. 2) has been divided into a number of terranes (Drury and De Souza, 1998), in a  
318 similar manner to its Saudi Arabian equivalent (Johnson et al., 2011). We suggest that these  
319 terranes formed a complex middle Tonian continental amalgam.

320

321 The older, Tonian to earliest Cryogenian, amalgamation history of the ANS is marked by  
322 approximately ENE-WSW oriented sutures (present orientation) between juvenile  
323 Neoproterozoic ocean-arc terranes (Collins et al., 2021a; Collins et al., 2021b)(Fig. 2). The oldest  
324 of these sutures is between the Jiddah-Haya and Gabgaba/Gebeit-Hijaz terranes (the Bi'r Umq–  
325 Nakasib suture)("bu" in Fig. 2), which is dated at ca. 780–750 Ma (Johnson et al., 2011). This  
326 suture created the kernel of a late Tonian microcontinent. The Midyan-Eastern Desert terrane  
327 collided with this kernel ca. 715 Ma along the Yanbu-Sol Hamed suture (Robinson et al., 2015a)  
328 ("y" in Fig. 2). Both sutures evolved from SE-dipping subduction zones (Robinson et al., 2015a).

329

330 The older ENE–WSW sutures are bound by younger NNW–SSE oriented Cryogenian to Ediacaran  
331 sutures and terranes that represent a fundamental kinematic change in Mozambique Ocean  
332 subduction (Collins et al., 2021a; Collins et al., 2021b). The oldest of these is the 680–640 Ma  
333 Nabitah suture (Flowerdew et al., 2013)("ns" in Fig. 2), which forms the eastern margin of the  
334 intra-Mozambique Ocean island-arc terrane microcontinent (discussed above), against Tonian-  
335 Cryogenian continental arcs (Siham and Suwaj arcs of Kashghari et al., 2025)("SK" and "Sj" in Fig.  
336 2) built on the Afif-Abas microcontinent. This now Cryogenian engorged Afif-Abas  
337 microcontinent collided with the active margin of the Sahara basement along the Sudanese Keraf  
338 Suture ("ks" in Fig. 2). This collision occurred in late Cryogenian to early Ediacaran times (ca. 650–  
339 580 Ma)(Abdelsalam et al., 1998). Further to the east, in the most easterly exposed terrane—the  
340 Saudi Ar Rayn Terrane—juvenile calc-alkaline magmatism stretches from ca. 690 Ma to 615 Ma

341 (Doebrich et al., 2007). Turbiditic sediment deposition in the Ad Dawadmi basin (“AD” in Fig. 2)  
342 that separates the Ar Rayn Terrane (“AR” in Fig. 2) from the Afif-Abas microcontinent continued  
343 until at least 620 Ma (Cox et al., 2012), but was locally intruded by ca. 630 Ma adakitic magmas  
344 (Cox et al., 2019). This sequence was metamorphosed to greenschist-facies grades at ca. 620 Ma  
345 (Cox et al., 2012). Further east still, broad N–S magnetic highs, beneath the Arabian Phanerozoic  
346 sedimentary sequence (Johnson and Stewart, 1995), suggest younger arc terranes now buried  
347 beneath the Rub al-Khali Basin (Fig. 2). Geochronological data from basement-intercepting  
348 boreholes throughout Saudi Arabia exclusively yield Neoproterozoic ages from these buried  
349 terranes (Collins et al., 2024). Deformation that we interpret as related to the collision and  
350 amalgamation of these buried terranes is prominent in the subsurface of western Oman where  
351 it is known as the Western Deformation Front (“WDF” in Fig. 2) and delineates the Angudan  
352 Orogeny (Loosveld et al., 1996; Al-Barwani and McClay, 2008; Gómez-Pérez and Morton, 2025).  
353 Al Rawahi et al. (2026) demonstrated from provenance changes in the late Ediacaran Fara  
354 Formation of Oman that closure of this suture occurred by ca. 551 Ma. We correlate this latest  
355 Ediacaran–Cambrian Angudan orogeny with the Malagasy orogeny of Collins and Pisarevsky  
356 (2005). This event is interpreted as the final suture of the Mozambique Ocean (Gómez-Pérez et  
357 al., 2024; Gómez-Pérez and Morton, 2025). A zone of lithospheric mantle shear wave anisotropy  
358 in far southwestern Oman may locate this suture in the upper mantle (Al-Lazki et al., 2012), this  
359 broadly correlates with highly strained Ediacaran volcano-clastics found in the subsurface and at  
360 outcrop (Gómez-Pérez and Morton, 2025). The transition to post-tectonic magmatism within the  
361 eastern terranes of the Arabian Nubian Shield begins from ca. 605 Ma with post-tectonic  
362 magmatism (Doebrich et al., 2007; Cox et al., 2012; Robinson et al., 2014; Robinson et al., 2015b;  
363 a; Cox et al., 2019) and pull-apart basins developed along the large strike-slip faults (known as  
364 the Najd Faults) that cut the region (Moore, 1979; Meyer et al., 2014; Nettle et al., 2014; Shen et  
365 al., 2022; Hamimi et al., 2023).

366

367 The basement of Yemen is marked by considerable pre-Neoproterozoic crust found in the Al-  
368 Mahfid and Abas terranes (Windley et al., 1996; Whitehouse et al., 1998). The Abas terrane is  
369 linked with the Siham-Khida terrane of Saudi Arabia (Whitehouse et al., 1998; Yeshanew et al.,

370 2015) to form the Afif-Abas continent of Collins and Pisarevsky (2005)(Fig. 2). Whereas the Al-  
371 Mahfid terrane has been linked with pre-Stenian crust found through Somaliland, eastern  
372 Ethiopia, southern Somalia, central Madagascar and the Madurai Block of southern India that  
373 formed the continent Azania (Whitehouse et al., 2001; Collins and Pisarevsky, 2005). The Abas  
374 Terrane lies east of an interpreted late Tonian to Cryogenian arc, called the Amlah Terrane  
375 (Whitehouse et al., 2025)("Aml" in Fig. 2) and an oceanic suture between this and the Saudi  
376 Arabia Tathlith terrane (Kashghari et al., 2025) is inferred by the change in younging direction of  
377 preserved volcanic arc intrusions (Flowerdew et al., 2013; Whitehouse et al., 2025). The Abas  
378 terrane is largely composed of ca. 790–725 Ma granitic gneisses with variable  $\epsilon(\text{Nd})_t$  values as  
379 evolved as -11, suggesting significant ancient crust in the source magmas (Whitehouse et al.,  
380 1998; Yeshanew et al., 2015). Some rocks may date back to the early Tonian and a single  
381 Neoproterozoic core has been analysed hinting at the age of older basement (Whitehouse et al.,  
382 1998). The juvenile Al Bayda terrane ("ABa" in Fig. 2) separates the Abas terrane from the Al  
383 Mahfid terrane. The latter contains significant Neoproterozoic crust and was interpreted by Collins  
384 and Windley (2002) to form the northern part of a Neoproterozoic continent that lies within the  
385 EAO (Azania of Collins and Pisarevsky, 2005). The Al Mukalla terrane ("Amk" in Fig. 2) lies east of  
386 the Al Mahfid in Yemen and was correlated by Whitehouse et al. (2001) with the Maydh (or Mait)  
387 terrane of northern Somalia (Somaliland)("M" in Fig. 2), which contains meta-tholeiitic basalts  
388 with pillow-lavas textures and mid-ocean ridge like chemistries (Dal Piaz et al., 1993).

389

390 Pre-Neoproterozoic rocks are found along the southern escarpment margin of the Gulf of Aden  
391 in northern Somalia (Somaliland) and eastern Ethiopia form a > 600 km long inlier between the  
392 latitudes of 41–47° E, from Hirna in east Ethiopia to the town of Maydh in northern Somalia.  
393 These were included within Azania by Collins and Pisarevsky (2005). In Somaliland, the oldest  
394 components of this inlier are the Qabri Bahar and Mora complexes (Sassi et al., 1993)("QM" in  
395 Fig. 2), which consists of paragneisses and orthogneisses with local migmatites and granulite-  
396 facies relics (Sassi and Visonà, 1993). The east Ethiopian continuation of this belt makes-up the  
397 unimagatively named 'Lower Unit' and Bora Group of the Harar-Hirna area (Kazmin, 1975;  
398 Berhe, 1981)("HH" in Fig. 2) that contain ca. 2000 Ma tonalitic gneiss xenoliths in Tonian

399 granitoids (Teklay et al., 1998; Yeshanew et al., 2017). In addition, Archaean and earliest  
400 Palaeoproterozoic zircon grains have been reported from granitoids interleaved with  
401 metasedimentary gneisses (Teklay et al., 1998). All analysed rocks in eastern Ethiopia have  
402 evolved neodymium isotope values, suggesting that either there are older rocks at depth, or the  
403 a sedimentary source was derived from more ancient crust, or both (Teklay et al., 1998;  
404 Yeshanew et al., 2017).

405  
406 In Eritrea, the Tokar/Barka terrane (Johnson and Woldehaimanot, 2003) consists of juvenile 850–  
407 650 Ma old supracrustal and intrusive rocks that range from low greenschist facies to granulite  
408 facies (Andersson et al., 2006). Peak metamorphism of these rocks is dated at ca. 590 Ma  
409 (Andersson et al., 2006). Rocks of the Tokar/Barka terrane in Eritrea pass south into the Tsaliet  
410 Group of Tigray in northern Ethiopia where they conformably pass up into Tonian strata of the  
411 Tambien Group that are well dated to between ca. 820 Ma and < 719 Ma (Swanson-Hysell et al.,  
412 2015; Park et al., 2019). This region has missed the high-grade Ediacaran metamorphism seen  
413 both to the east and west.

414  
415 To the southwest, the Western Ethiopian Shield (WES) is one of the larger regions of ANS outcrop  
416 (Fig. 2). It marks the transition from the relatively low-grade ANS to the higher metamorphic  
417 grades of the Mozambique Belt (Abdelsalam and Stern, 1996). The WES preserves no evidence  
418 of pre-Neoproterozoic crust, with the oldest rocks in the area dated at ca. 855 Ma (Blades et al.,  
419 2015) with geochemical evidence suggesting that they formed above an intra-oceanic subduction  
420 zones (Blades et al., 2019). Magmatism (re-melting of juvenile crust) and deformation is seen at  
421 810–770 Ma and at 660–635 Ma in the Western Ethiopian Shield, with post tectonic magmatism  
422 at ca. 584 Ma (Blades et al., 2015; Blades et al., 2019; Bowden et al., 2020). All the rocks in the  
423 Western Ethiopian Shield have juvenile  $\epsilon\text{Hf}(t)$  values of +4.5 to +10, suggesting that the influence  
424 of continental crust was minimal.

425

## 426 **THE WESTERN MARGIN OF THE EAST AFRICAN OROGEN**

427 ***Sudan, Chad, Central African Republic, South Sudan, Uganda***

428

429 The western margin of the East African Orogen can be reasonably well located in northern Sudan  
430 where > 900 Ma schists and gneisses are overthrust by 800–900 Ma gneisses and low-grade  
431 metavolcanic rocks of the Rahaba–Absol terrane (Harms et al., 1994; Schandelmeier et al., 1994;  
432 Johnson and Woldehaimanot, 2003)(“RA” in Fig. 2). Thrusting was over here before 700 Ma  
433 (Abdelsalam et al., 1995). As you get further south, though, the western margin becomes hard to  
434 locate as much of the south-east of the region often denoted as the Sahara Metacraton  
435 (Abdelsalam et al., 2002) has a basement made up of late Mesoproterozoic rocks that formed in  
436 volcanic arc terranes (Shellnutt et al., 2017; Blades et al., 2020; Djerosse et al., 2020; Plunder  
437 et al., 2026). This suggests that this part of the basement to Chad and Sudan forms an earlier  
438 accretionary orogen that simply gets younger eastward into the EAO—part of a large and long-  
439 lived accretionary system, possibly stretching to the eastern edge of the West African Craton  
440 (Şengör et al., 2020; Lom et al., 2024; Shellnutt et al., 2026).

441

442 The Nuba Mountains lie at a critical point to the west of the traditional western boundary of the  
443 EAO, yet north of the Ediacaran tectonism that marks the Central African Fold Belt (Fig. 2). The  
444 eastern part of the exposed basement rocks consist of low-grade volcano-sedimentary rocks that  
445 are separated from a higher-grade gneiss terrane in the central Nuba Mountains by the Kabus  
446 ophiolitic mélange (Abdelsalam and Dawoud, 1991). This boundary has long been used to mark  
447 the western boundary of the ANS and therefore the East African Orogen (Abdelsalam and  
448 Dawoud, 1991; Johnson and Woldehaimanot, 2003). Mohammed (2017), however, showed that  
449 these gneisses are Neoproterozoic and to the west of them lies a ca. 780 Ma ophiolitic succession  
450 that he named the Arid Unit. This suggests that juvenile Neoproterozoic crust continues west of  
451 the Nuba Mountains and that these mountains lie close to the triple junction where the EAO  
452 meets the Central African Fold Belt (Fig. 2).

453

#### 454 **THE NORTHEASTERN EAST AFRICAN OROGEN**

455 ***NW India, Pakistan, Oman, UAE, Afghanistan, SE China, Seychelles, N Madagascar***

456

457 There are three main windows into the Omani basement exposed east of the ‘Western  
458 Deformation Front’. These all lie east of the possible lithospheric suture marked by shear wave  
459 splitting in far southwestern Oman (Al-Lazki et al., 2012). The tectonic windows are Al Jobah  
460 (northern Huqf area), Jebel Ja’Alan (NE Oman) and Mirbat region of Dhofar in the south-east  
461 (“Hu”, “JJ” and “Mir” in Fig. 2). These have been interpreted to represent arc accretion during  
462 the Tonian (890–720 Ma) (Stern and Johnson, 2010; Rantakokko et al., 2014; Whitehouse et al.,  
463 2016; Alessio et al., 2018), with magmatism and deformation/metamorphism broadly younging  
464 from the NE to the SW, towards the putative final Mozambique Ocean suture (Blades et al., 2020).  
465 In addition, clasts brought up from > 8km depth in salt diapirs in Oman and the United Arab  
466 Emirates preserve volcanic rocks with ages between 560–545 Ma that contain inherited zircons  
467 back to the Neoproterozoic (Thomas et al., 2015). Detrital zircons in sedimentary enclaves show a  
468 similar age range (Thomas et al., 2015; Arboit et al., 2024) as do in-situ metasedimentary  
469 basement rocks of the Jebel Ja’Alan region (Whitehouse et al., 2016; Blades et al., 2020). These  
470 suggest a depositional connection to crust of considerable antiquity. A number of workers have  
471 suggested that Afghanistan may be possible source for these (Thomas et al., 2015; Alessio et al.,  
472 2018; Blades et al., 2020), as this Archaean/Palaeoproterozoic terrane likely lay with the NW  
473 Neoproterozoic Indian accretionary system and was interpreted in Merdith et al. (2021) as  
474 correlating with the SW of the Yangtze craton of China as a microcontinent accreted to the  
475 Neoproterozoic Indian margin in the Tonian.

476

477 In Gondwana, Oman lay adjacent to NW India in Gondwana (Figs. 1, 2), and by Ediacaran times,  
478 at least, a similar sedimentary package was deposited across Rajasthan, Pakistan and through  
479 Oman that contains excellent petroleum source rocks and evaporites (Cozzi et al., 2012). These  
480 were being deposited in a stable, passive margin environment (Allen, 2007) at the same time that  
481 rocks in the eastern Saudi Arabian Shield were forming in an active subduction margin (Cox et al.,  
482 2012). The pre-Ediacaran basement rocks in Rajasthan and Pakistan, also, share similarities with  
483 those of Oman. Granitoids have been dated from Rajasthan (“Raj” in Fig. 2) and from Nagar  
484 Parkar in eastern Sind (Pakistan, “NP” in Fig. 2) at ca. 1.1 Ga (Raza et al., 2012; Meert et al., 2013).  
485 But no evidence of pre-existing crust occurs west of the Western Margin Fault of the Aravalli-

486 Delhi Orogen (“wmf” in Fig. 2). Tonian granitoids and rhyolites occur in inliers through northwest  
487 India and Pakistan, where they cluster into crystallization ages of ca. 990–970 Ma (Pandit et al.,  
488 2003), ca. 860–820 Ma (Davies and Crawford, 1971; Deb et al., 2001; Van Lente et al., 2009; Just  
489 et al., 2011) and ca. 775–760 Ma (Gregory et al., 2009; Van Lente et al., 2009; Ashwal et al., 2013;  
490 Meert et al., 2013). The latter magmatic and extrusive phase forms one of the largest felsic  
491 igneous provinces on the planet, which is also traced to the Seychelles (Torsvik et al., 2001;  
492 Tucker et al., 2001)(“Sey” in Fig. 2), and may correlate with the northern Bemarivo Belt of  
493 Madagascar where the magmatism dates from ca. 750–705 Ma (Collins, 2006; Thomas et al.,  
494 2009; Armistead et al., 2019)(“Bem” in Fig. 2).

495  
496 Armistead et al. (2019), showed that ca. 750–705 Ma rocks from the northern Bemarivo Belt of  
497 far north Madagascar preserve similar juvenile  $\epsilon\text{Hf}(t)$  signatures to rocks in south China,  
498 Rajasthan, Oman and the Seychelles, that had previously been suggested to have formed a  
499 volcanic arc system on the margin of Neoproterozoic India (Wang et al., 2017; Cawood et al.,  
500 2018). The period of magmatism in this proposed arc was long-lived, beginning at around ca. 850  
501 Ma and ending at around ca. 700 Ma. When reconstructed in this fashion (Armistead et al., 2019),  
502 there is a general southward to southeastward younging trend (reconstructed orientation), with  
503 the oldest record coming from China, and progressing to younger rocks through Oman, Malani,  
504 Seychelles and the northern Bemarivo Belt.

505  
506 Tonian palaeomagnetic data from Oman (Swanson-Hysell et al., 2025; Antonio et al., 2026)  
507 support the correlation of Oman with Neoproterozoic India at the time (Alessio et al., 2018).  
508 Sedimentological data from the Cryogenian and Ediacaran deposits suggest that this link lasts  
509 through until Ediacaran formation of Gondwana (Cozzi et al., 2012; Gómez-Pérez et al., 2024;  
510 Gómez-Pérez and Morton, 2025). Only colliding with the rest of Arabia in the late Ediacaran  
511 (Collins and Pisarevsky, 2005; Blades et al., 2020; Merdith et al., 2021; Cao et al., 2024; Gómez-  
512 Pérez and Morton, 2025; Al Rawahi et al., 2026).

513

514 **THE CENTRAL EAST AFRICAN OROGEN**

515 ***Southern Ethiopia, Uganda, Kenya, NE Tanzania, southern Somalia***

516

517 The grade of metamorphism of rocks exposed on the surface increases through Ethiopia from  
518 the broadly greenschist-facies rocks of the ANS in the north to upper amphibolite and granulite-  
519 grade rocks that dominate the Mozambique Belt south of central Ethiopia. We interpret this  
520 transition to reflect greater Cryogenian to Cambrian orogenesis in the south with higher and  
521 more extensive orogenic topography of the overlying mountains (see discussion below for more  
522 on palaeoelevation).

523

524 South of the Western Ethiopian Shield (WES, Fig. 2), the Karamoja Belt of NE Uganda (“Kmja” in  
525 Fig. 2) is dominated by the Karasuk Supergroup (Vail, 1985; Westerhof et al., 2014), which are  
526 metaigneous rocks that crystallized between ca. 740 Ma and ca. 680 Ma (Mänttari et al., 2011;  
527 Westerhof et al., 2014) and are intruded by post-tectonic granitoids with U–Pb crystallization  
528 ages of ca. 660 Ma (Mänttari et al., 2011). Similar timing of magmatism is seen within the WES  
529 (Blades et al., 2015), however, there is a notable difference between the Southern Ethiopian  
530 Shield (“SES” in Fig. 2) and the Karamoja Belt. In the Southern Ethiopian Shield, a ca. 660 Ma  
531 event that is coeval with the late magmatism in the eastern WES, is termed the ‘Moyale Event’  
532 (Teklay et al., 1998) this is associated with multiply deformed dismembered ophiolites (Abebe et  
533 al., 2025). Further east still, Yeshanew et al. (2017) identified Ediacaran granitic magmatism (600  
534 – 560 Ma) in the Harar region of eastern Ethiopia (“HH” in Fig. 2). The Ediacaran ages extend  
535 known magmatic events in the region to much younger ages than previously reported, and  
536 considerably younger than any orogenesis in the Western Ethiopian Shield. Two of the granitoid  
537 samples dated at ca. 600 and ca. 585 Ma are not deformed, whereas the younger gneisses at ca.  
538 568 and ca. 560 Ma are strongly deformed. These were interpreted to represent a low-strain  
539 domain during orogenesis (Yeshanew et al., 2017) and suturing between two lithospheric blocks  
540 (WES and Eastern Ethiopia—Azania?). These mid-late Ediacaran ages are much younger than any  
541 evidence for tectonism found in the WES, and any suggested ocean closure from the ANS west  
542 of the Saudi Arabian Afif Terrane (Johnson et al., 2011), so rather than representing suturing  
543 between the WES and eastern Ethiopia, we suggest that the post-ca. 560 Ma deformation may

544 reflect late intra-continental deformation, as seen elsewhere in the ANS (e.g., Kusky and Matsah,  
545 2003).

546

547 To the south, in Kenya, southern Somalia and Tanzania, the East African Orogen is dominated by  
548 high-grade gneisses of the Mozambique Belt (see Fritz et al., 2013 for a review)(“Moz Belt” in Fig.  
549 2). In the region of the town of Lodwar in NW Kenya (“Ld” in Fig. 2), amphibolite-grade  
550 orthogneisses yield protolith ages of ca. 800 Ma that were metamorphosed at ca. 630 Ma (Blades  
551 et al., 2026). These are separated from the NE edge of the Congo-Tanzania-Bangweulu Block by  
552 the Cryogenian to early Ediacaran West Pokat ophiolite (Vearncombe, 1983; Ries et al.,  
553 1992)(“Pok” in Fig. 2) and are themselves bound to the east by metasedimentary gneisses that  
554 record peak metamorphic conditions of 8.4–10.6 kbar and temperatures of 750–830°C at ca. 625  
555 Ma (McIntyre, 2023). The Lodwar orthogneisses likely correlate north with the Didesa Terrane  
556 (West Ethiopian Shield; Blades et al., 2015). This region passes south into the Western Granulites  
557 of SW Kenya and Tanzania (“WG” in Fig. 2) that involve highly metamorphosed pre-  
558 Neoproterozoic crust that was metamorphosed to granulite facies at ca. 630–615 Ma (Möller et  
559 al., 2000; Sommer et al., 2003; Cutten et al., 2006; Apen et al., 2020) and locally extruded  
560 westward over the Congo-Tanzania-Bangweulu Block (Eguíluz et al., 2024).

561

562 The eastern part of the Mozambique Belt (Burr Massif, Somalia, Fig. 2) consists of a tract of largely  
563 pre-Neoproterozoic continental crust, strongly deformed, partially melted and metamorphosed  
564 in the Ediacaran/Cambrian (ca. 600 and ca. 530 Ma, Küster et al., 1990; Lenoir et al., 1994).  
565 Extensive tectonothermally reworked pre-Neoproterozoic crust lies further west in the  
566 Neoproterozoic Tanzanian craton (Muhongo et al., 2001; Johnson et al., 2003; Reddy et al., 2003;  
567 Tenczer et al., 2013). Near peak, granulite-grade metamorphism along the western part of this  
568 belt (ca. 640 Ma), has been dated by metamorphic zircons (Coolen et al., 1982; Muhongo, 1994;  
569 Appel et al., 1998; Muhongo et al., 2001). Hauzenberger et al. (2007) identified that the age of  
570 metamorphism further east, in the Galana River area (“GR” in Fig. 2), is considerably younger  
571 (580–530 Ma) overlapping the age of the ‘Malagasy Orogeny’ of Collins and Pisarevsky (2005).

572

573 **THE SOUTHERN EAST AFRICAN OROGEN: THE MOZAMBIQUE BELT AND THE EAST AFRICAN**  
574 **OROGEN BIFURCATION**

575 *Tanzania, northern Mozambique, Madagascar*

576

577 In Gondwana, Madagascar lay directly off the east coast of Tanzania and SE Kenya (Reeves et al.,  
578 2004)(Figs. 1, 2). Terranes in this area have been tentatively extended into western Madagascar  
579 (Fritz et al., 2013). For example, in the South Kenyan Galana River region, the Sobo Unit has been  
580 correlated with the pre-Neoproterozoic terranes of western Madagascar, while the Galana and  
581 Sagala Units are linked with the Vohibory Terrane of far SW Madagascar (Fritz and Hauzenberger,  
582 2021)(“V” in Fig. 2). The Rantosara shear zone of southern Madagascar also has been correlated  
583 with deformation along the Galana-Mutito Shear Zone (Hauzenberger et al., 2007). Unlike the  
584 Ranotsara shear zone (“rsz” in Fig. 2), though, the Galana-Mutito Shear Zone separates distinct  
585 terranes with different protolith origins and histories (Schreurs et al., 2010; Fritz et al., 2013; Fritz  
586 and Hauzenberger, 2021). To the east of the Galana-Mutito Shear Zone lies the microcontinent  
587 Azania (Fig. 2), whereas to the west are a series of Neoproterozoic terranes known as the Kasigau  
588 and Kurase Units in Kenya (Frisch and Pohl, 1986), the Eastern Granulites in Tanzania (Maboko,  
589 2000)(“EG” in Fig. 2) and the Cabo Delgado Nappe Complex in northern Mozambique (Viola et  
590 al., 2008)(“CD” in Fig. 2). These originated as Neoproterozoic volcanic arcs that consumed the  
591 western branch of the Mozambique Ocean (Kröner et al., 2003; Cutten et al., 2006; Mole et al.,  
592 2018; Fritz and Hauzenberger, 2021).

593

594 Subduction of a strand of the Mozambique Ocean that separated the  
595 Congo/Tanzania/Bangweulu continent from Azania began as early as 1080 Ma with the formation  
596 of an intra-oceanic volcanic arc that is preserved today as the ca. 1080–980 Ma Dabolava Arc of  
597 western Madagascar (Tucker et al., 2014; Archibald et al., 2018)(“Db” in Fig. 2). This arc system  
598 can be traced south in reconstructed Gondwana into the ‘Tonian Oceanic Arc Superterrane’  
599 (TOAST) region of East Antarctica (Jacobs et al., 2015; Merdith et al., 2017b; Merdith et al.,  
600 2021)(Fig. 2). Later formed, early Tonian, supra-subduction arc systems included magmatism on  
601 the surrounding pieces of continental crust as well as within the ocean itself. These include the

602 Galana and Sagala units with emplacement ages between 970 Ma and 850 Ma and the ca. 930–  
603 900 Ma Vohibory arc terrane of SW Madagascar (Jöns et al., 2005; Jöns and Schenk, 2008; Collins  
604 et al., 2012)(Fig. 2). Protoliths to granulites in the Pare–Usambara and Uluguru Mountains (“Ulu”  
605 in Fig. 2) of Eastern Tanzania preserve subduction-related magmatism dated to ca. 700–800 Ma,  
606 which is broadly coeval with the extensive 850–750 Ma Itsindro-Imerona arc that intruded  
607 throughout central Madagascar (Handke et al., 1997; Archibald et al., 2016; Archibald et al.,  
608 2017). Finally, the youngest known subduction-arc terrane in this area forms the ca. 700–650 Ma  
609 Ntaka terrane of southern Tanzania (Mole et al., 2018)(“Nt” in Fig. 2).

610  
611 In Madagascar, accreted Late Mesoproterozoic to Tonian arc systems make up much of the  
612 western part of the exposed basement of the island (Collins, 2006; Tucker et al., 2014; Archibald  
613 et al., 2018; Boger et al., 2019; Collins et al., 2022a). The central part of Madagascar (the  
614 Antananarivo Domain, “Tana” in Fig. 2) forms a pre-Neoproterozoic continent made up of  
615 Archaean orthogneisses (Tucker et al., 1999; Tucker et al., 2011; Armistead et al., 2018; Archibald  
616 et al., 2023), overlain and interleaved with Palaeoproterozoic and Mesoproterozoic sequences of  
617 meta-sedimentary rocks (Cox et al., 1998; Cox et al., 2004; Boger et al., 2014b; Archibald et al.,  
618 2015; Armistead et al., 2021; Costa et al., 2021). To the east of this pre-Neoproterozoic unit lies  
619 a series of Neoproterozoic metasedimentary rocks that include pods of ultramafic rocks (the  
620 Anaboriana-Manampotsy belt). These rocks separate central Madagascar from the Antongil and  
621 Masora domains (“At” and “Ms” in Fig. 2, respectively); the former, at least, is a displaced part of  
622 the Western Dharwar Craton (Tucker et al., 1999; Tucker et al., 2014; Armistead et al., 2018).  
623 Collins et al. (2003) suggested that the Anaboriana-Manampotsy belt forms a cryptic suture (the  
624 Betsimisaraka Suture, “bet” in Fig. 2) between a Neoproterozoic continent (named 'Azania' by  
625 Collins and Pisarevsky, 2005) and Neoproterozoic India (Collins and Windley, 2002). This  
626 interpretation was countered by Tucker et al. (2011; 2014) who argued that central Madagascar  
627 was a continuation of the Dharwar Craton and that the Anaboriana-Manampotsy belt originated  
628 as an intra-continental basin. The Anaboriana-Manampotsy belt passes north to the Bemarivo  
629 Domain of far north Madagascar (Collins and Windley, 2002)(“Bem” in Fig. 2). Here, Armistead et  
630 al. (2019) demonstrated that the northern part of this region formed a juvenile ca. 750–700 Ma

631 terrane that they named the Bobakindro Terrane. These authors argued that it formed a  
632 continuation of the volcanic arc terranes that accreted to Neoproterozoic India during the Tonian  
633 and Cryogenian (Blades et al., 2020; Collins et al., 2021b) and correlated south with the  
634 Betsimisaraka Suture to separate Neoproterozoic India from Azania and African-derived terranes.

635  
636 The foreland to the Lurio Belt of northern Mozambique consists of the Stenian Nampula Complex  
637 (“Na” in Fig. 2), which is relatively weakly deformed and metamorphosed in the Neoproterozoic  
638 (Kroner et al., 1997; Sacchi et al., 2000; Bingen et al., 2009). The Lurio foreland disrupts the  
639 orogenic trend of the EAO and splits it into southwestern and southeastern branches with a triple  
640 junction that lay directly south of Madagascar and Southern India (Schmitt et al., 2018; Clark et  
641 al., 2020)(Figs. 1, 2). The southwestern branch passes through Malawi and as it tracks further  
642 west, it is progressively known as the Zambezi Belt, the Lufilian Arc (Fig. 2) and eventually the  
643 Central Damara Orogen in Namibia (“Da” in Fig. 1). The southeastern branch forms a broad  
644 orocline, curving through Sri Lanka where it encompasses the Wannian and Highland Complexes  
645 (“W” and “HC” in Fig. 2, respectively). The orocline wraps around the Stenian Vijayan Complex  
646 (correlated with the Nampula Complex by Collins and Pisarevsky, 2005)(“V” in Fig. 2) and passes  
647 into East Antarctica in the region of Lutzöw Holm Bay (“Lut” in Fig. 2).

648

## 649 **THE SOUTHWEST BRANCH OF THE EAST AFRICAN OROGEN**

### 650 ***Northern Mozambique, Malawi, Zambia***

651 Northern Mozambique and southeastern Zambia experienced extension and deposition in the  
652 early Neoproterozoic. Metasedimentary units in the Marrupa and Unango complexes of  
653 Mozambique (Bingen et al., 2009)(“M-U” in Fig. 2) and the Nyimba-Sinda Terrane of Zambia  
654 (Alessio et al., 2019a)(“N-S” in Fig. 2) likely reflect basin development contemporaneous with late  
655 Tonian/early Cryogenian rift-related magmatism in NE Mozambique (Bjerkgaard et al., 2009),  
656 Malawi (Ashwal et al., 2007) and east Zambia (Johnson et al., 2006). This rifting is interpreted as  
657 associated with the breakup of central Rodinia and connected with the initial opening of the  
658 Pacific Ocean basin (Merdith et al., 2017a). Subsequent collision between the Kalahari continent  
659 and the Congo-Tanzania-Bangweulu Block formed some of the younger orogenesis that made-

660 up Gondwana (Schmitt et al., 2018; Gomes et al., 2025). Peak metamorphism within the central  
661 Damara Orogen (“Da” in Fig. 1) culminated at 530–525 Ma (Goscombe et al., 2017), which  
662 matches similar Cambrian peak metamorphism in the Zambezi Belt (John et al., 2004). Post-peak  
663 cooling was well underway through much of the belt by the end of the Cambrian (Alessio et al.,  
664 2019b; Vincent et al., 2026).

665

## 666 **THE SOUTHEAST BRANCH OF THE EAST AFRICAN OROGEN**

### 667 ***South India, Sri Lanka, East Antarctica***

668 Southern India has been divided into a series of tectonic units with distinct protolith origins and  
669 tectonothermal histories. From north to south these are: the Salem Block (sometimes called the  
670 Northern Granulite Terrane); the Palghat-Cauvery shear system (“pcss” in Fig. 2); the Madurai  
671 Block (“Mad” in Fig. 2); the Achancovil Zone (“asz” in Fig. 2); the Trivandrum Block (also known  
672 as the Kerala Khondalite Belt); and the Nagercoil Block (both amalgamated as “TN” in Fig. 2) (e.g.  
673 Santosh et al., 2009; Collins et al., 2014). The Palghat-Cauvery shear system has long been noted  
674 to separate autochthonous parts of Neoproterozoic India from more exotic terranes to the south  
675 (Bartlett et al., 1998; Cenko et al., 2004; Collins et al., 2014; Plavsa et al., 2015).

676

677 The northwest of the Madurai Block is composed of charnockite massifs with Sm–Nd and Rb–Sr  
678 whole rock model ages in the range of 3170–2200 Ma (Bartlett et al., 1998; Bhaskar Rao et al.,  
679 2003). U–Pb zircon ages from charnockites in this northwest Madurai Block have yielded a  
680 consistent range of crystallisation ages between ca. 2.55 and 2.50 Ga (Ghosh et al., 2004; Brandt  
681 et al., 2011; Plavsa et al., 2012). This northern region is separated from the rest of the  
682 predominantly metasedimentary Madurai Block first by a lithological boundary that broadly  
683 follows the Karur-Kamban-Painavu-Trichur lineament (known as the KKPT) (Ghosh et al., 2004)  
684 that can also be seen as a zone of S-dipping reflectors in deep seismic surveys (Rajendra Prasad  
685 et al., 2007). South of the KKPT (“kkpt” in Fig. 2) is a broad zone of highly deformed and  
686 metamorphosed Archaean/Palaeoproterozoic metasedimentary rocks that continue until a line  
687 approximately from Rajapalayam to Madurai (Plavsa et al., 2014; Kumar et al., 2017).  
688 Neoproterozoic metasedimentary rocks with Mesoproterozoic to Neoproterozoic metaigneous

689 plutons that have continental arc-like chemistries dominate the region south of this  
690 Rajapalayam–Madurai line and pass into the Achankovil Zone where Neoproterozoic rocks are  
691 deformed into a prominent SE–NW striking high strain zone (Guru Rajesh and Chetty, 2006).

692  
693 Some workers have subdivided the southern part of Kerala and Tamil Nadu into the Trivandrum  
694 and Nagercoil Blocks (Santosh et al., 2003; Santosh et al., 2006). U–Pb zircon data from the  
695 charnockites that are common in the region demonstrate that both blocks preserve similar ages  
696 and really seem to be differentiated just on the dominance of charnockite in the Nagercoil Block  
697 and metasedimentary rocks in the Trivandrum Block (Cenki et al., 2004; Kröner et al., 2012;  
698 Johnson et al., 2015; Kumar et al., 2017; Clark et al., 2020). The metaigneous protoliths formed  
699 at ca. 2040 Ma in an oceanic magmatic arc setting and are distinct from elsewhere in southern  
700 India, but likely correlate with the basement of the Androyen and Anosyen terranes of southern  
701 Madagascar (Tucker et al., 2014), possibly the Highland Complex of Sri Lanka (Kitano et al., 2018)  
702 and even with parts of East Africa (Clark et al., 2020). The area including all these regions, with  
703 the exception of East Africa, was named “SMIWH” (South Madagascar, India, Wannan-Highland  
704 Complex) by Tucker et al. (2014), who argued that this terrane accreted to the Dharwar Craton  
705 by the late Palaeoproterozoic. We note that this terrane is separated from the pre-1000 Ma crust  
706 of India by the Neoproterozoic southern Madurai and Achankovil terranes (Plavsa et al., 2012;  
707 Plavsa et al., 2015), which leads us to disagree with the proposed Palaeoproterozoic accretion  
708 and suggest that this terrane combined with cratonic India during the Ediacaran high-grade  
709 metamorphism seen throughout the region (Collins et al., 2007; Clark et al., 2009; Collins et al.,  
710 2014; Taylor et al., 2014; Plavsa et al., 2015). We also point out that no reliable evidence exists  
711 for pre-Stenian basement in the Sri Lankan Wannan Complex, and that it shouldn’t be considered  
712 part of this terrane; the acronym SMIWH then is inaccurate.

713  
714 We suggest that the contiguous Gondwanan terrane encompassing the Androyen/Anosyen  
715 domains of Madagascar, the Trivandrum Block of southmost India and the Highland Complex of  
716 Sri Lanka be called ‘Pandya’ after i) the named used for the metamorphic belt of southern India

717 (Pandyan Mobile Belt, Ramakrishnan, 1993), ii) the ancient Tamil dynasty of southern India,  
718 whose lands encompassed parts of Sri Lanka at their greatest extent.

719

## 720 **DISCUSSION**

### 721 ***The Plate Tectonic Evolution of the East African Orogen***

722 The tectonic geography represented by the various terranes of the East African Orogen can be  
723 difficult to deduce where extreme metamorphism and deformation has transposed all physical  
724 evidence and often rendered geochemical evidence enigmatic. Such obfuscation is a particular  
725 challenge in the southern East African Orogen—a region known as the Mozambique Belt (Fritz et  
726 al., 2013). Along orogenic strike, though, outcrop metamorphic grade decreases towards the  
727 north—from granulite and upper amphibolite grade rocks in the southern EAO to greenschist  
728 facies and sub-greenschist facies rocks preserved in the northern parts of the EAO . By  
729 comparison, in the northern EAO most surface rocks experienced metamorphism of no more  
730 than greenschist-facies and original sedimentary/volcanic features are commonly preserved as  
731 are near-original chemistries of the rocks. It is here in the Arabian-Nubian Shield where many  
732 pre-continent/continent collision tectonic events that affected the region can be best defined  
733 (Johnson et al., 2011; Collins et al., 2021a; Collins et al., 2021b).

734

### 735 ***The East African Orogen—the Largest Mountain Belt of the Last Billion Years?***

736 There is a good case to suggest that the EAO is the largest collisional orogen of the last billion  
737 years simply based on its footprint on a reconstructed Gondwana. Extending across  
738 approximately 100 degrees of longitude at low to moderate southern latitudes (Collins et al.,  
739 2021b) the orogen was over 10,000 kms long and extend over 1000 km at its widest point (in the  
740 region now preserved in Mozambique, Madagascar and Southern India)(Figs. 1, 2). The scale is  
741 comparable to the modern Alpine-Himalaya chain, and like this modern orogen, the EAO was  
742 large enough to strongly change the oceanic radiogenic strontium isotopic curve (Chen et al.,  
743 2022). In fact, global ocean  $^{87}\text{Sr}/^{86}\text{Sr}$  values only rise dramatically twice in the last billion years;  
744 once from 50 Ma to present, due to erosion of the growing Himalaya, and in the late  
745 Neoproterozoic (Chen et al., 2022). Zhu et al. (2022) looked at the scale of orogens through time

746 from a different perspective. By examining the rare earth element chemistry of dated detrital  
747 zircons, they showed that there are two main times of ‘supermountain’ formation, one in the  
748 Palaeoproterozoic and a second contemporaneous with the EAO. The youth of the Himalayan  
749 orogen is the likely reason for no significant record of it in these detrital zircons. Therefore, as  
750 well as the EAO (along with contemporaneous Gondwana-forming orogens in Africa and South  
751 America) being of a scale to affect ocean water composition, it also thickened the crust enough  
752 to significantly affect the trace-element chemistry of zircon-producing magmas. This suggests  
753 that the orogen was not only spatially extensive, but also formed mountains of an elevation at  
754 least as high as those seen in Asia today. As proposed by Zhu et al. (2022), erosion of this  
755 ‘supermountain’ would likely stimulate biological productivity and widely effect the wider  
756 planetary system (e.g., Squire et al., 2006; Halverson et al., 2010). The orogen’s broad E–W  
757 orientation and location in relatively low to moderate latitudes likely accentuated its erosion and  
758 multiplied its effect on other Earth systems (in a similar manner to the Late Palaeozoic orogens  
759 demonstrated by Godderis et al., 2017). Merdith et al. (Submitted) demonstrated the importance  
760 of this within a computational whole-Earth, where they traced the evolution of tectonic plate  
761 boundaries, to automatically isolate specific tectonic environments that are associated with  
762 mountain building, such as continental arcs, continental collisions, rifts and large igneous  
763 provinces. From this they simulated orogenic growth, and erosion, over the last 1 Ga, using  
764 parameters and limits derived from the present-day expression of topography on Earth to  
765 provide a quantitative and tractable basis for palaeoclimate or landscape evolution modelling  
766 over the last 1 Ga. This semi-automated topography model uses ‘rules’ relating orogenic  
767 topography to the nature and location of plate boundaries. The next step is to use geological data  
768 to constrain topographic evolution directly from nature.

769

770 To obtain a better understanding of the role the EAO plays in the tumultuous changes to the  
771 climate, biosphere and atmosphere in the Neoproterozoic an understanding of the spatial and  
772 temporal evolution of elevation through the orogen is needed. Unravelling topography from the  
773 now denuded and dispersed remains of the East African Orogen mountains is a complex task. We  
774 have taken the approach here of mapping pressure and time determinations from the literature

775 on a reconstruction of Gondwana (Merdith et al., 2021). We limit our analyses to exclude low  
776 geothermal gradient metamorphism (< 450 K/GPa) as this is usually interpreted as subduction-  
777 zone related (Brown and Johnson, 2019). In this situation, pressure (depth) will not necessarily  
778 relate to surface elevation due to the non-isostatic nature of these environments. We have also  
779 ignored the possible effects of differential stress (Schmalholz and Podladchikov, 2014;  
780 Tajčmanová et al., 2021; Zuza et al., 2022) due to the difficulty of quantifying its effect on mean  
781 stress, metamorphic determinations (pressure).

782

783 A simple isostatic correction to present day elevation can be produced from metamorphic  
784 pressure estimates to estimate palaeo-elevation (Fig. 3). Given a peak metamorphic pressure,  
785  $P_s$ , at the time of metamorphism, the height of eroded material,  $h$ , can be estimated from an  
786 assumed density ( $2850 \text{ kg m}^{-3}$ ) for the eroded material,  $\rho$ , and gravity,  $g$ , by

$$787 \quad h = \frac{P_s}{\rho g}.$$

788 Assuming the lower crust and mantle lithosphere at the time of metamorphism is the same  
789 today, their contributions cancel out of the isostatic balance; thus mantle density,  $\rho_m$ , and  
790 present day elevation,  $\varepsilon_{pd}$  are the only additional parameters needed to compute the elevation  
791 at the time of peak metamorphism,  $\varepsilon_{EAO}$ . Using the local isostatic balance equations: (1)  $\rho h =$   
792  $\rho_m h_m$  and (2)  $h = h_m + \varepsilon_{EAO} - \varepsilon_{pd}$ , where  $h_m$  is the thickness of mantle needed to compensate  
793 the change in load, we estimate the palaeo-elevation by,

$$794 \quad \varepsilon_{EAO} = \varepsilon_{pd} + \frac{P_s}{\rho g} \left( 1 - \frac{\rho}{\rho_m} \right).$$

795

796 A total of 197 metamorphic conditions have been compiled (Table 1), supplementing the P–T  
797 database by Brown and Johnson (2019). Present-day elevation was determined by averaging  
798 pixels in a 25 km radius about the sample location, though in many cases locations are  
799 approximated from a map or description. While it is beyond the scope of this study to produce  
800 a rigorous elevation model, which ideally would incorporate thermal effects and compositional  
801 uncertainties (Hasterok and Chapman, 2007), where pressure ranges have been provided an  
802 elevation range was computed (Table 1).

803

804 Predicted elevations range from near sea-level to a maximum of ca. 10 km, with an average of  
805  $5.1 \pm 1.6$  km, similar in elevation to the modern Tibetan Plateau, and over a similar area (Figs. 1,  
806 5). The modelled EAO palaeo-elevations are greater than the global average palaeo-elevations  
807 (Fig. 4) and are normally distributed. One may expect a more exponential distribution for  
808 elevation, though it is unsurprising that elevation predicted from peak metamorphic pressures  
809 does not. The primary reason for this difference is the lack of precise recording of pressures at  
810 low metamorphic grades, which are difficult due to kinetic rates at low temperatures. Hence our  
811 estimates likely yield elevation estimates in the orogenic plateau and range crest (Fig. 5). Since  
812 there is no obvious decrease in elevation at the eastern and western edges of the plateau, the  
813 area of elevated terrain is likely much greater than the distribution of model estimates.

814

815 Based on these simple elevation estimates, we suggest that the high topography varied spatially  
816 in time as the orogen evolved. High elevations were created in the first phase of the orogen  
817 (680–640 Ma; i.e. the East African Orogeny of Collins and Pisarevsky, 2005), recorded as high  
818 elevations > 6 km in the Tanzanian Eastern Granulites associated with shortening during  
819 subduction and collision of Azania with the Congo-Tanzania-Bangweulu Block (Fig. 5). In the  
820 second phase (640–580 Ma), the elevation remained high in the Mozambique Belt and southern  
821 Azania. At this time, many regions in the Arabian-Nubian Shield also reached peak metamorphic  
822 pressure conditions, though at lower maxima that result in a lower topography (~ 2.5–4 km, Fig.  
823 5 and Table 1). The final stage of the EAO (The Malagasy Orogeny of Collins and Pisarevsky, 2005)  
824 resulted in the development of an extensive orogenic plateau, with the highest modelled  
825 elevations (8–10 km) in the south, in present-day coastal East Antarctica, and throughout a broad  
826 plateau that extended from the margin of the Congo–Tanzania–Bangweulu continent, across  
827 Azania in present-day Madagascar, Sri Lanka and the Southern Granulite Terrane of India (Figs.  
828 1, 2, 5). It is unlikely that the highest elevations are accurate as regional compensation would  
829 likely have resulted in lower elevations, however, we assert that the aerial extent of the high  
830 elevations in the plateau regions is reasonable, i.e., within the bounds of elevation observed in  
831 Tibet and the Himalaya today (Fig. 4). On the basis of these estimates, we suggest that the EAO  
832 was amongst the largest, highest mountain belts known on Earth, rivalling the Alpine-Himalayan

833 Orogen of today and lending support to hypotheses that have the orogen fundamental to earth  
834 surface systems tipping points, such as facilitating carbon burial and planetary oxygenation that  
835 are broadly coeval with the orogen's apogee (e.g., Zhu et al., 2022).

836

837 ***Suggestions for further work***

838

839 A grand challenge of earth science is to be able to map the evolution of Earth's surface systems  
840 through its history. This is a herculean task, but a worthy task, as it is only by developing a deeper  
841 understanding of the geological record that can drive more naturalistic models of the planet that  
842 we can understand how our planet works, and how the geosphere interacts with the atmosphere  
843 to develop the climate, hydrosphere and biosphere (e.g., Mills et al., 2025). Developing a model  
844 of the Earth system over the ca. 500 million years of the Neoproterozoic involves reconstructing  
845 both the plate tectonic evolution of the planet, and the evolution of the planet's surface  
846 elevation.

847

848 The reconstruction presented here (Figs. 1, 2), and the palaeo-geographically controlled palaeo-  
849 elevation estimates (Fig. 5), are only the first attempt at integrating the full plate tectonic record  
850 with the metamorphic record to track the evolution of this one (albeit large) mountain range.  
851 Much of the geology of the East African Orogen is poorly known, especially when compared with  
852 that of Phanerozoic mountain ranges such as the European Alps, North American Appalachians  
853 or Chinese Qinling mountains. Much work is needed to unravel the paleo-plate tectonic evolution  
854 of the orogen, especially in the countries of east and northeast Africa, Arabia, Madagascar, South  
855 Asia and East Antarctica. This is in addition to the other Neoproterozoic orogens that lace South  
856 America, Australia and parts of Asia.

857

858 We hope to have demonstrated that when triaged carefully, the metamorphic record preserves  
859 palaeo-topographic information that is difficult to recover by other methods. We note that much  
860 of the available metamorphic record through Proterozoic orogens is governed by point analyses  
861 on restricted outcrops where high variance lithologies occur that are used to constrain the

862 pressure-temperature and time evolution of that one location. We encourage future pressure-  
863 time campaign-style studies that may be able to determine the geometry of orogenic topography  
864 and along-strike variations that will considerably improve the resulting models.

865  
866 As an example of what is possible. We undertook a reconnaissance pressure-time study of  
867 southern India that was reported in Collins et al. (2022b). Here we dated garnets using the in-situ  
868 Lu-Hf technique over an orogenic transect (Tamblyn et al., 2022) and examined the trapped  
869 pressures of quartz inclusions using RAMAN spectroscopy to obtain peak pressures. Many  
870 exhumed orogens are garnet-rich and a similar approach could be done through many of the  
871 Proterozoic orogens to better understand their topographic evolution.

872  
873 The answer in the end involves a community-wide approach to supporting geological research  
874 globally, and especially in the global south. Then integrating plate-tectonic reconstructions  
875 developed from these works into a global reconstruction. Topography can then be added by  
876 combining estimates of past elevation from the proximity of a region to a plate boundary (in the  
877 style of Meredith et al., Submitted) with estimates from geochemistry of igneous rocks (e.g. Zhu  
878 et al., 2022; Zhou et al., 2025) and estimates from the metamorphic record as discussed here.

879

## 880 **CONCLUSIONS**

881 The East African Orogen is one of the largest known orogens on the planet, on a similar, or greater  
882 scale, than the present-day Alpine-Himalaya orogen. Reconstructions of the orogen show that it  
883 not only bisected Gondwana, but it also developed a thick orogenic plateau that rivals Tibet for  
884 elevation and area (Fig. 1). The East African Orogen evolved from a Mesoproterozoic accretionary  
885 orogen that developed to the east of the West African Craton and north of the Congo-Tanzania-  
886 Bangweulu Block. Throughout the Tonian accretionary orogenesis characterized the orogen with  
887 considerable volcanic-arc development on the margins of the growing nuclei of Africa (soon to  
888 be central Gondwana) and within the Mozambique Ocean. The collision of Azania (and other  
889 intra-Mozambique Ocean continents) with the active margin of Africa caused an early continent-

890 continent collisional orogeny—the East African Orogeny. This was later followed by the Ediacaran  
891 collision of Neoproterozoic India with the growing kernel of central Gondwana.

892

893 The available metamorphic record supports the designation of the East African Orogen as, if not  
894 the largest, then one of the largest mountain ranges in Earth history (Fig. 4). Past ground  
895 elevation estimates constructed from the triaged metamorphic record are located on the full-  
896 plate tectonic reconstruction of Cao et al. (2024), which is fundamentally based on Merdith et al.  
897 (2021), and reveals the elevation consequences of the series of plate-tectonic events (Fig. 4). This  
898 also demonstrates the along-strike variability along the orogen, with contemporary palaeo-  
899 elevations in the Arabian-Nubian Sheild region being considerably lower than in the Mozambique  
900 Belt, reflecting the geometry and kinematics of the plate-movements at the time. Our plate-  
901 tectonic/palaeo-elevation approach is suggested as a way forward in reconstructing the shape of  
902 the Earth in deep time—a key parameter in future earth systems models of the planet.

903

#### 904 **ACKNOWLEDGMENTS**

905 ASC and MLB are funded by Australian Research Council grants FL240100114 and DP250102570.  
906 ASM is funded by DE230101642. ASC thanks the numerous colleagues and students who have  
907 assisted on the projects that led to his fascination with the East African Orogen and the formation  
908 of Gondwana.

909

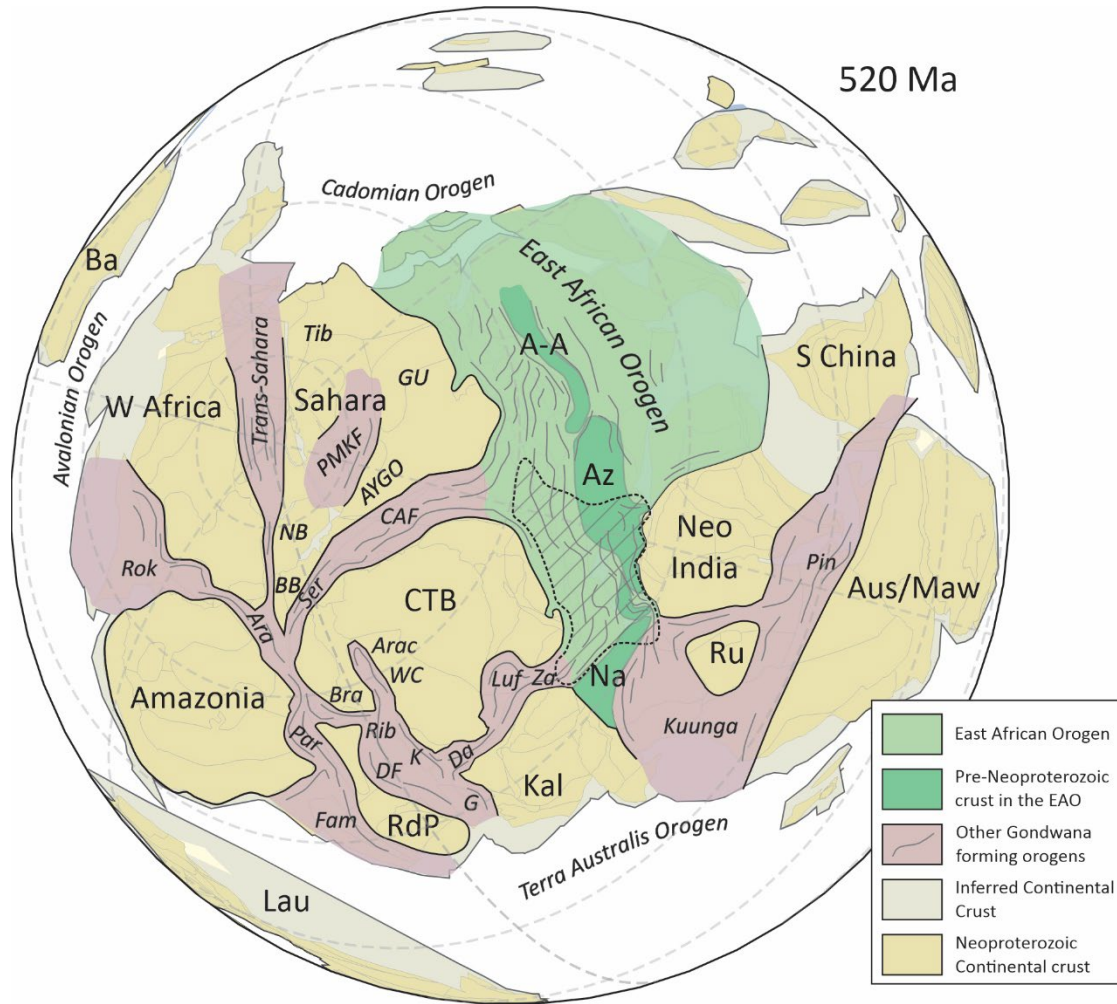
910

911 **Table 1 - Peak metamorphic conditions and model paleo elevations within the East African Orogen.**

912 **(see spreadsheet).**

913

914 **FIGURE CAPTIONS**



915

916

917 Figure 1: Reconstruction of Gondwana in the early Cambrian (520 Ma), after Merdith et al. (2021)

918 with the East African Orogen (EAO) outlined along with major regions of Pre-Neoproterozoic

919 crust reworked within the EAO; A-A = Afif-Abas Terrane, Az = Azania, Na = Nampula Terrane.

920 Other major Gondwana-forming orogens are outlined, which are; Ara = Araguaia Belt, Arac =

921 Aracuaí Orogen, Bra = Brasília Belt, CAF = Central African Fold Belt, Da = central Damara Belt, DF

922 = Dom Feliciano Belt, Fam = Famatinian Orogen, G = Gariep Belt, K = Kaoko Belt, Kuunga = Kuunga

923 Orogen, Luf = Lufilian Arc, Par = Paraguay Belt, Pin = Pinjarra Orogen, Rib = Ribeira Belt, Rok =

924 Rokelide Orogen, Ser = Sergipano Orogen, Trans-Sahara = Trans-Saharan Orogen, WC = West

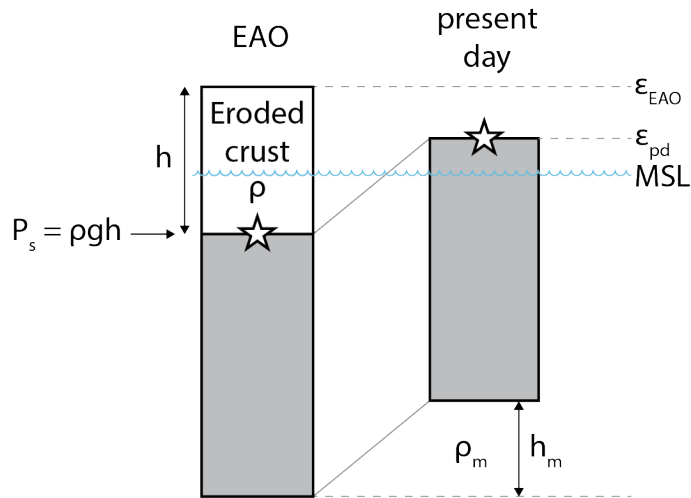
925 Congo Orogen, Za = Zambezi Belt. The major Neoproterozoic continental blocks are; Aus/Maw =

926 Australia/Mawson Continent, Ba = Baltica, CTB = Congo-Tanzania-Bangweulu (also includes the  
927 São Francisco craton of Brazil), GU = Gebel Uweinat, Kal = Kalahari, Lau = Laurentia, Neo India =  
928 Neoproterozoic India, PMKF = Poli-Mayo Kebbi-Lake Fitri Terrane, W Africa = West Africa  
929 (including the São Luis Block of Brazil), RdP = Río de la Plata (and including the putative  
930 Paranapanema craton), Ru = Ruker Terrane (likely a continuation of Neoproterozoic India),  
931 Sahara = Saharan basement (including the Nigeria-Benin block [NB], the Brazilian Borborema  
932 Province [BB], Tibesti [Tib], Gebel Uweinat [GU] and the Adamawa-Yadé-Guéra-Ouaddaï Terrane  
933 [AYGO]), S China = South China. The broad sites where three of the Gondwana-peripheral  
934 orogens will form are also marked, these are the Avalonian Orogen, the Cadomian Orogen, and  
935 the Terra Australia Orogen. The cross-hatched zone in the EAO is where the highest-grade  
936 metamorphic rocks from the East African orogen and Malagasy orogens are found, which  
937 approximates to the position of the Mozambique Belt and forms the past position of the large  
938 orogenic plateau discussed in this paper. Broad orogenic strike lines are added within the  
939 Gondwana-forming orogens.



943 (tectonised) in the Neoproterozoic, or formed in the Neoproterozoic, are coloured shades of  
944 green. Abbreviations used are: AA = Anosyen-Andasibe domains, Ab = Abas terrane, ABa = Al  
945 Bayda terrane, AD = Ad Dawadmi terrane, AMa = Al Mafid terrane, Amk = Al Mukalla terrane,  
946 Aml = Amlah terrane, AN = An Nimas terrane, AR = Ar Rayn terrane, At = Antongil Domain, Bem  
947 = Bemarivo Belt (the Bobakindro terrane is the northernmost part of this belt), Bi = Bidah terrane,  
948 CD = Cabo Delgado Complex, Db = Dabolava Suite (arc), Did = Didesa terrane, ED = Eastern Desert  
949 of Egypt, EG = Eastern Granulites, GG = Gabgaba/Gebeit terrane, GR = Galana River, H = Haya  
950 terrane, HC = Highland Complex, HH = Harar-Hirna, Hi = Hijaz terrane, Hu = Huqf, J = Jiddah  
951 terrane, JJ = Jebel Ja'alan, Kmja = Karamoja Belt, Ld = Lodwar, Lut = Lutzöw-Holm Bay, M = Maydh  
952 (or Mait) complex, Mad = Madurai Block, Mid = Midyan terrane, Mir = Mirbat, Ms = Masora  
953 Domain, M-U = Marrupa-Unango complexes, Nam = Nampula Complex, NP = Nanga Parkar, N-S  
954 = Nyimba-Sinda Terrane, Nt = Ntaka terrane, NUBA = Nuba Mountains, QAM = Al Qarah-Malahah  
955 terrane, QM = Qabri Bahar and Mora complexes, RA = Rahaba-Absol terrane, Raj = Rajasthan,  
956 Ray = Rayner Complex, Ruk = Ruker domain, Sa'al = Sa'al Metamorphic Complex, Sahara =  
957 Sarahan basement (including pre-Neoproterozoic crustal terranes and Neoproterozoic juvenile  
958 terranes), SES = Southern Ethiopian Shield, Sey = Seychelles, Sj = Suwaj, SK = Siham-Khida terrane,  
959 Soc = Socotra, Ta = Tathlith terrane, Tana = Antananarivo Domain, TB = Tokar/Barka terrane, TN  
960 = Trivandrum-Nagercoil blocks, Ulu = Uluguru Mountains, V = Vohibory Domain, Vj = Vijayan  
961 Complex, W = Wannu Complex, WES = Western Ethiopian Shield, WG = Western Granulites, Y-Y  
962 Yaoundé-Yangana nappes. Shear zones and sutures are marked with the following acronyms; asz  
963 = Achancovil shear zone, bet = Betsimisaraka Suture (in the Anaboriana-Manampotsy belt), bu =  
964 Bi'r Umq suture, kkpt = Karur-Kamban-Painavu-Trichur lineament, ks = Keraf Suture, nak =  
965 Nakasib suture, ns = Nabitah suture, pok = West Pokat suture, pcss = Palghat-Cauvery Shear  
966 System, rsz = Ranotsara shear zone, sh = Sol-Hamed Suture, wmf = Western Margin Fault, y =  
967 Yanbo suture.

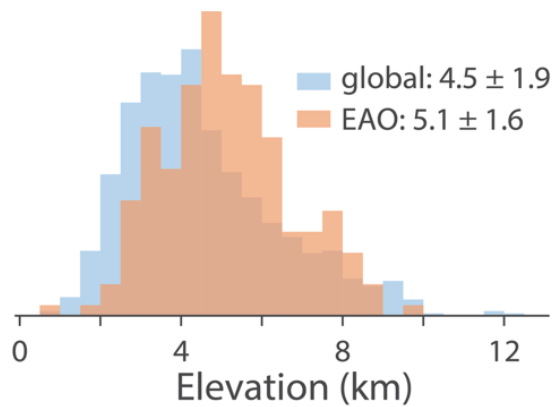
968



969

970 Figure 3: Isostatic columns used to estimate elevation during the East African Orogen from  
 971 metamorphic pressure estimates. Isostatic column during the East African Orogen (left) included  
 972 overburden that eroded (average density,  $\rho$ , and thickness,  $h$ ), exposing the metamorphic  
 973 pressure ( $P_s$ , star) at present day (right).

974

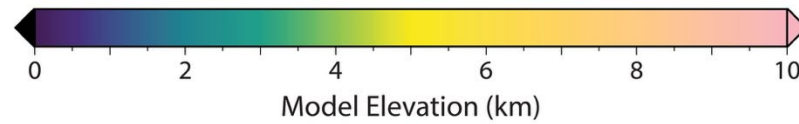
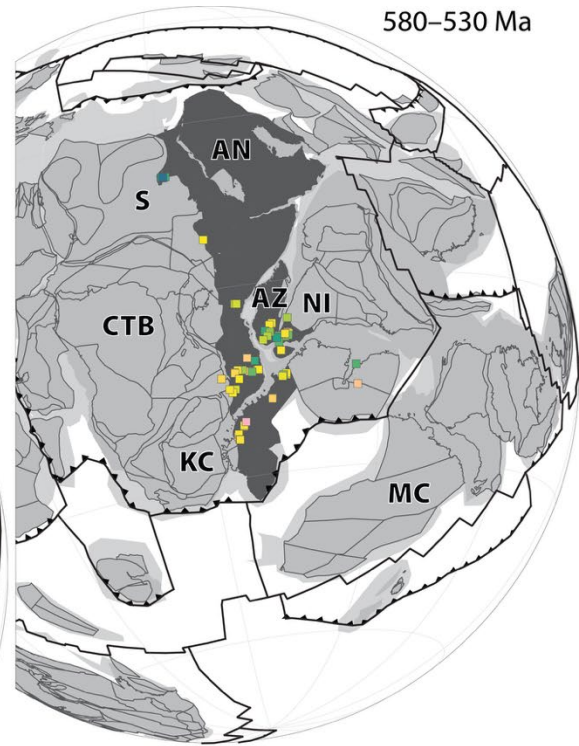
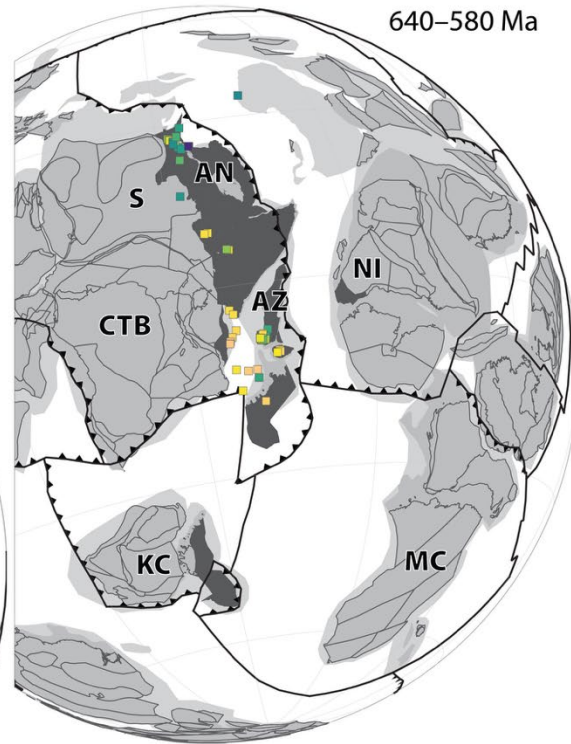
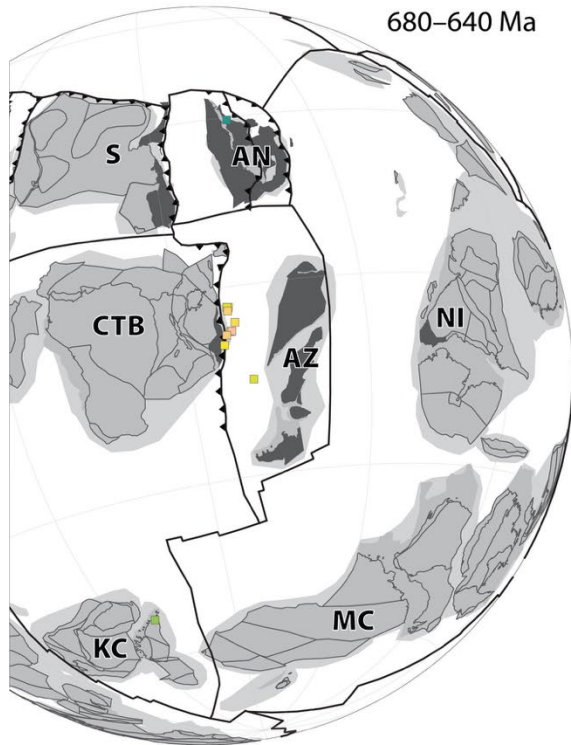


975

976 Figure 4: Palaeo-elevation estimates for the East African Orogen (EAO) compared to the global  
 977 dataset excluding EAO data. Individual palaeo-elevation estimates are provided in Table 1. The  
 978 global estimates are derived from pressures included in an expanded metamorphic database  
 979 originally by Brown and Johnson (2019)). Data were prefiltered for metamorphic pressures  
 980 below 2 GPa and metamorphic thermal gradients above 450 K/GPa to remove most subduction-  
 981 related events.

982

AN - Arabia–Nubia  
 AZ - Azania  
 CTB - Congo–Tanzania–Bangweulu Continent  
 KC - Kalhari Continent  
 MC - Mawson Continent  
 NI - Neoproterozoic India  
 S - Saharan Metacraton



984 Figure 5: Palaeo-elevation estimates for the East African Orogen. The P–T locations have been  
985 reconstructed from the tectonic model by Cao et al. (2024) at time steps 660, 600, and 550 Ma,  
986 corresponding to the palaeo-elevation estimates at 680–640, 640–580, and 580–520 Ma,  
987 respectively. The plate models are fixed relative to the Congo-Tanzania-Bangweulu Block.

988

## 989 REFERENCES CITED

990

- 991 Abdelsalam, M.G. and Dawoud, A.S., 1991. The Kabus ophiolitic melange, Sudan, and its  
992 bearing on the western boundary of the Nubian Shield. *Journal of the Geological Society*,  
993 London, 148: 83-92.
- 994 Abdelsalam, M.G., Liegeois, J.P. and Stern, R.J., 2002. The Saharan Metacraton. *Journal of*  
995 *African Earth Sciences*, 34(3-4): 119-136.
- 996 Abdelsalam, M.G. and Stern, R.J., 1996. Sutures and shear zones in the Arabian-Nubian Shield.  
997 *Journal Of African Earth Sciences*, 23(3): 289-310.
- 998 Abdelsalam, M.G., Stern, R.J., Copeland, P., El-Faki, E.-F.M., Al-Hur, B. and Ibrahim, F.M.,  
999 1998. The Neoproterozoic Keraf Suture in NE Sudan: sinistral transpression along the  
1000 eastern margin of West Gondwana. *Journal of Geology*, 106: 133-147.
- 1001 Abdelsalam, M.G., Stern, R.J., Schandelmeier, H. and Sultan, M., 1995. Deformation history of  
1002 the Keraf Zone in NE Sudan, revealed by Shuttle Imaging Radar. *Journal of Geology*,  
1003 103: 475–491.
- 1004 Abebe, E., Alene, M., Tesfaw, B., Sano, T. and Kusaba, Y., 2025. Structural and metamorphic  
1005 evolution of Neoproterozoic rocks in Bensa-Girja area, southern Ethiopia. *Journal of*  
1006 *African Earth Sciences*, 230.
- 1007 Al-Barwani, B. and McClay, K., 2008. Salt tectonics in the Thumrait area, in the southern part of  
1008 the South Oman Salt Basin: Implications for mini-basin evolution. *Georabia*, 13: 77-  
1009 108.
- 1010 Al-Lazki, A., Ebinger, C., Kendall, M., Helffrich, G., Leroy, S., Tiberi, C., Stuart, G. and Al-  
1011 Toobi, K., 2012. Upper mantle anisotropy of southeast Arabia passive margin [Gulf of  
1012 Aden northern conjugate margin], Oman. *Arabian Journal of Geosciences*, 5(5): 925-934.
- 1013 Al Rawahi, H., Gómez-Pérez, I., Bergmann, K.D., McCabe, R. and Cantine, M.D., 2026. Syn-  
1014 tectonic deposition during final closure of the Mozambique Ocean: the Ediacaran Fara  
1015 Formation in northern Oman. *Precambrian Research*, 442: 108095.
- 1016 Alessio, B.L., Blades, M.L., Murray, G., Thorpe, B., Collins, A.S., Kelsey, D.E., Foden, J.,  
1017 Payne, J., Al-Khribash, S. and Jourdan, F., 2018. Origin and tectonic evolution of the NE  
1018 basement of Oman: a window into the Neoproterozoic accretionary growth of India?  
1019 *Geological Magazine*, 155(5): 1150-1174.
- 1020 Alessio, B.L., Collins, A.S., Siegfried, P., Glorie, S., De Waele, B., Payne, J. and Archibald,  
1021 D.B., 2019a. Neoproterozoic tectonic geography of the south-east Congo Craton in  
1022 Zambia as deduced from the age and composition of detrital zircons. *Geoscience*  
1023 *Frontiers*, 10(6): 2045-2061.
- 1024 Alessio, B.L., Glorie, S., Collins, A.S., Jourdan, F., Jepson, G., Nixon, A., Siegfried, P.R. and  
1025 Clark, C., 2019b. The thermo-tectonic evolution of the southern Congo Craton margin as

1026 determined from apatite and muscovite thermochronology. *Tectonophysics*, 766: 398-  
1027 415.

1028 Allen, P.A., 2007. The Huqf Supergroup of Oman: Basin development and context for  
1029 Neoproterozoic glaciation. *Earth Science Reviews*, 84: 139-185.

1030 Anders, B., Reischmann, T., Kostopoulos, D. and Poller, U., 2006. The oldest rocks of Greece:  
1031 first evidence for a Precambrian terrane within the Pelagonian Zone. *Geological*  
1032 *Magazine*, 143(1): 41-58.

1033 Andersson, U.B., Ghebreab, W. and Teklay, A., 2006. Crustal evolution and metamorphism in  
1034 east-central Eritrea, south-east Arabian-Nubian Shield. *Journal of African Earth Sciences*,  
1035 44(1): 45-65.

1036 Antonio, P.Y.J., Rousse, S., Macouin, M., Ganerod, M., Roques, D., Denèle, Y. and Benoit, M.,  
1037 2026. East side story of Gondwana: the last frontier of the Arabian Nubian shield at 720  
1038 Ma based on new high-quality paleomagnetic pole. *Gondwana Research*, 149: 113-126.

1039 Apen, F.E., Rudnick, R.L., Cottle, J.M., Kylander-Clark, A.R.C., Blondes, M.S., Piccoli, P.M.  
1040 and Seward, G., 2020. Four-dimensional thermal evolution of the East African Orogen:  
1041 accessory phase petrochronology of crustal profiles through the Tanzanian Craton and  
1042 Mozambique Belt, northeastern Tanzania. *Contributions to Mineralogy and Petrology*,  
1043 175(11).

1044 Appel, P., Möller, P. and Schenk, V., 1998. High-pressure granulite facies metamorphism in the  
1045 Pan-African belt of eastern Tanzania: P-T-t evidence against granulite formation by  
1046 continent collision. *Journal of Metamorphic Geology*, 16: 491-509.

1047 Arboit, F., Ceriani, A., Collins, A., Hennhofer, D., Pilia, S. and Decarlis, A., 2024. The tectonic  
1048 setting of the late Ediacaran eastern Arabian basement (ca. 550 Ma): New  
1049 geochronological and geochemical constraints from the basements of Oman and the  
1050 United Arab Emirates. *Gondwana Research*, 130: 203-219.

1051 Archibald, D.B., Collins, A.S., Armistead, S.E., Foden, J.D., Payne, J.L. and Razakamanana, T.,  
1052 2023. Zircon U–Pb, oxygen, and hafnium isotopic characteristics of the Neoproterozoic–  
1053 Palaeoproterozoic Betsiboka Suite, Madagascar: tracing source to sink pathways in  
1054 Proterozoic and Phanerozoic provenance studies. *Geological Society, London, Special*  
1055 *Publications*, 531(1): SP531-2022-162.

1056 Archibald, D.B., Collins, A.S., Foden, J.D., Payne, J.L., Holden, P., Razakamanana, T., De  
1057 Waele, B., Thomas, R.J. and Pitfield, P.E.J., 2016. Genesis of the Tonian Imorona-  
1058 Itsindro magmatic Suite in central Madagascar: Insights from U-Pb, oxygen and hafnium  
1059 isotopes in zircon. *Precambrian Research*, 281: 312-337.

1060 Archibald, D.B., Collins, A.S., Foden, J.D., Payne, J.L., Macey, P.H., Holden, P. and  
1061 Razakamanana, T., 2018. Stenian-Tonian arc magmatism in west-central Madagascar: the  
1062 genesis of the Dabolava Suite. *Journal of the Geological Society*, 175(1): 111-129.

1063 Archibald, D.B., Collins, A.S., Foden, J.D., Payne, J.L., Taylor, R., Holden, P., Razakamanana,  
1064 T. and Clark, C., 2015. Towards unravelling the Mozambique Ocean conundrum using a  
1065 triumvirate of zircon isotopic proxies on the Ambatolampy Group, central Madagascar.  
1066 *Tectonophysics*, 662: 167-182.

1067 Archibald, D.B., Collins, A.S., Foden, J.D. and Razakamanana, T., 2017. Tonian Arc  
1068 Magmatism in Central Madagascar: The Petrogenesis of the Imorona-Itsindro Suite.  
1069 *Journal of Geology*, 125(3): 271-297.

1070 Armistead, S.E., Collins, A.S., Merdith, A.S., Payne, J.L., Cox, G.M., Foden, J.D.,  
1071 Razakamanana, T. and De Waele, B., 2019. Evolving Marginal Terranes During

1072 Neoproterozoic Supercontinent Reorganization: Constraints From the Bemarivo Domain  
1073 in Northern Madagascar. *Tectonics*, 38(6): 2019-2035.

1074 Armistead, S.E., Collins, A.S., Payne, J.L., Foden, J.D., De Waele, B., Shaji, E. and Santosh, M.,  
1075 2018. A re-evaluation of the Kumta Suture in western peninsular India and its extension  
1076 into Madagascar. *Journal of Asian Earth Sciences*, 157: 317-328.

1077 Armistead, S.E., Collins, A.S., Schmitt, R.S., Costa, R.L., De Waele, B., Razakamanana, T.,  
1078 Payne, J.L. and Foden, J.D., 2021. Proterozoic Basin Evolution and Tectonic Geography  
1079 of Madagascar: Implications for an East Africa Connection During the Paleoproterozoic.  
1080 *Tectonics*, 40(3): e2020TC006498.

1081 Ashwal, L.D., Armstrong, R.A., Roberts, R.J., Schmitz, M.D., Corfu, F., Hetherington, C.J.,  
1082 Burke, K. and Gerber, M., 2007. Geochronology of zircon megacrysts from nepheline-  
1083 bearing gneisses as constraints on tectonic setting: implications for resetting of the U-Pb  
1084 and Lu-Hf isotopic systems. *Contributions to Mineralogy and Petrology*, 153(4): 389-  
1085 403.

1086 Ashwal, L.D., Solanki, A.M., Pandit, M.K., Corfu, F., Hendriks, B.W.H., Burke, K. and Torsvik,  
1087 T.H., 2013. Geochronology and geochemistry of Neoproterozoic Mt. Abu granitoids, NW  
1088 India: Regional correlation and implications for Rodinia paleogeography. *Precambrian  
1089 Research*, 236: 265-281.

1090 Bartlett, J.M., Dougherty-Page, J.S., Harris, N.B.W., Hawkesworth, C.J. and Santosh, M., 1998.  
1091 The application of single zircon evaporation and model Nd ages to the interpretation of  
1092 polymetamorphic terrains: an example from the Proterozoic mobile belt of south India.  
1093 *Contributions to Mineralogy and Petrology*, 131: 181-195.

1094 Be'eri-Shlevin, Y., Eyal, M., Eyal, Y., Whitehouse, M.J. and Litvinovsky, B., 2012. The Sa'al  
1095 volcano-sedimentary complex (Sinai, Egypt): A latest Mesoproterozoic volcanic arc in  
1096 the northern Arabian Nubian Shield. *Geology*, 40(5): 403-406.

1097 Be'eri-Shlevin, Y., Katzir, Y., Whitehouse, M.J. and Kleinhanns, I.C., 2009. Contribution of pre  
1098 Pan-African crust to formation of the Arabian Nubian Shield: New secondary ionization  
1099 mass spectrometry U-Pb and O studies of zircon. *Geology*, 37(10): 899-902.

1100 Berhe, S.M., 1981. The geology of the Dire Dawa area. Memoir of the Ethiopian Institute of  
1101 Geological Survey.

1102 Bhaskar Rao, Y.J., Janardhan, A.S., Vijaya Kumar, T., Narayana, B.L., Dayal, A.M., Taylor,  
1103 P.N. and Chetty, T.R.K., 2003. Sm-Nd model ages and Rb-Sr isotope systematics of  
1104 charnockites and gneisses across the Cauvery Shear Zone, southern India: implications  
1105 for the Archaean-Neoproterozoic boundary in the southern granulite terrain. In: M.  
1106 Ranmakrishnan (Editor), *Tectonics of Southern Granulite Terrain*. Geological Society of  
1107 India Memoir 50, pp. 297-317.

1108 Bingen, B., Jacobs, J., Viola, G., Henderson, I.H.C., Skar, O., Boyd, R., Thomas, R.J., Solli, A.,  
1109 Key, R.M. and Daudi, E.X.F., 2009. Geochronology of the Precambrian crust in the  
1110 Mozambique belt in NE Mozambique, and implications for Gondwana assembly.  
1111 *Precambrian Research*, 170(3-4): 231-255.

1112 Bjerkgard, T., Stein, H.J., Bingen, B., Henderson, I.H.C., Sandstad, J.S. and Moniz, A., 2009.  
1113 The Niassa Gold Belt, northern Mozambique - A segment of a continental-scale Pan-  
1114 African gold-bearing structure? *Journal of African Earth Sciences*, 53(1-2): 45-58.

1115 Blades, M.L., Alessio, B.L., Collins, A.S., Foden, J., Payne, J.L., Glorie, S., Holden, P., Thorpe,  
1116 B. and Al-Khirbash, S., 2020. Unravelling the Neoproterozoic accretionary history of

1117 Oman, using an array of isotopic systems in zircon. *Journal of the Geological Society*,  
1118 177(2): 357-378.

1119 Blades, M.L., Collins Alan, S., Boone, S., Ekai, F., McIntyre, A. and Wilson, K., 2026.  
1120 Unravelling the East African Orogen one terrane at a time: insights from NE Kenya,  
1121 Australian Earth Science Convention, Melbourne, pp. 231.

1122 Blades, M.L., Collins, A.S., Foden, J., Payne, J.L., Stüwe, K., Abu-Alam, T., Makroum, F. and  
1123 Hassan, M., 2021a. Age and hafnium isotope evolution of Sudanese Butana and Chad  
1124 illuminates the Stenian to Ediacaran evolution of the south and east Sahara. *Precambrian*  
1125 *Research*, 362: 106323.

1126 Blades, M.L., Collins, A.S., Foden, J., Payne, J.L., Xu, X.C., Alemu, T., Woldetinsae, G., Clark,  
1127 C. and Taylor, R.J.M., 2015. Age and hafnium isotopic evolution of the Didesa and  
1128 Kemashi Domains, western Ethiopia. *Precambrian Research*, 270: 267-284.

1129 Blades, M.L., Collins, A.S., Foden, J.D., Payne, J.L., Stüwe, K., Abu-Alam, T., Makroum, F. and  
1130 Hassan, M., 2021b. Age and hafnium isotope evolution of Sudanese Butana and Chad  
1131 illuminates the Stenian to Ediacaran evolution of the south and east Sahara. *Precambrian*  
1132 *Research*, 362: 106323.

1133 Blades, M.L., Foden, J., Collins, A.S., Alemu, T. and Woldetinsae, G., 2019. The origin of the  
1134 ultramafic rocks of the Tulu Dimtu Belt, western Ethiopia - do they represent remnants of  
1135 the Mozambique Ocean? *Geological Magazine*, 156(1): 62-82.

1136 Boger, S.D., Hirdes, W., Ferreira, C.A.M., Jenett, T., Dallwig, R. and Fanning, C.M., 2015. The  
1137 580-520 Ma Gondwana suture of Madagascar and its continuation into Antarctica and  
1138 Africa. *Gondwana Research*, 28(3): 1048-1060.

1139 Boger, S.D., Hirdes, W., Ferreira, C.A.M., Schulte, B., Jenett, T. and Fanning, C.M., 2014a.  
1140 From passive margin to volcano-sedimentary forearc: The Tonian to Cryogenian  
1141 evolution of the Anosyen Domain of southeastern Madagascar. *Precambrian Research*,  
1142 247: 159-186.

1143 Boger, S.D., Hirdes, W., Ferreira, C.A.M., Schulte, B., Jenett, T. and Fanning, C.M., 2014b.  
1144 From passive margin to volcano-sedimentary forearc: The Tonian to Cryogenian  
1145 evolution of the Anosyen Domain of southeastern Madagascar. *Precambrian Research*,  
1146 247: 159-186.

1147 Boger, S.D., Maas, R., Pastuhov, M., Macey, P.H., Hirdes, W., Schulte, B., Fanning, C.M.,  
1148 Ferreira, C.A.M., Jenett, T. and Dallwig, R., 2019. The tectonic domains of southern and  
1149 western Madagascar. *Precambrian Research*, 327: 144-175.

1150 Bowden, S., Gani, N.D., Alemu, T., O'Sullivan, P., Abebe, B. and Tadesse, K., 2020. Evolution  
1151 of the Western Ethiopian Shield revealed through U-Pb geochronology, petrogenesis, and  
1152 geochemistry of syn- and post-tectonic intrusive rocks. *Precambrian Research*, 338.

1153 Brandt, S., Schenk, V., Raith, M.M., P., A., Gerdes, A. and Srikantappa, C., 2011. Late  
1154 Neoproterozoic P-T evolution of HP-UHT granulites from the Palni Hills (South India):  
1155 New constraints from phase diagram modelling, LA-ICP-MS zircon dating and in-situ  
1156 EMP monazite dating. *Journal of Petrology*, 52: 1813-1856.

1157 Brown, M. and Johnson, T., 2019. Metamorphism and the evolution of subduction on Earth.  
1158 *American Mineralogist*, 104(8): 1065-1082.

1159 Burke, K., Dewey, J.F. and Kidd, W.S.F., 1976. Precambrian Paleomagnetic Results Compatible  
1160 with Contemporary Operation of Wilson Cycle. *Tectonophysics*, 33(3-4): 287-299.

1161 Candan, O., Koralay, O.E., Topuz, G., Oberhansli, R., Fritz, H., Collins, A.S. and Chen, F.,  
1162 2016. Late Neoproterozoic gabbro emplacement followed by early Cambrian eclogite-

1163 facies metamorphism in the Menderes Massif (W. Turkey): Implications on the final  
1164 assembly of Gondwana. *Gondwana Research*, 34: 158-173.

1165 Cao, X.Z., Collins, A.S., Pisarevsky, S., Flament, N., Li, S.Z., Hasterok, D. and Müller, R.D.,  
1166 2024. Earth's tectonic and plate boundary evolution over 1.8 billion years. *Geoscience*  
1167 *Frontiers*, 15(6).

1168 Cawood, P.A., 2005. Terra Australis Orogen: Rodinia breakup and development of the Pacific  
1169 and Iapetus margins of Gondwana during the Neoproterozoic and Paleozoic. *Earth*  
1170 *Science Reviews.*, 69: 249-279.

1171 Cawood, P.A. and Buchan, C., 2007. Linking accretionary orogenesis with supercontinent  
1172 assembly. *Earth Science Reviews.*, 82: 217-256.

1173 Cawood, P.A., Zhao, G.C., Yao, J.L., Wang, W., Xu, Y.J. and Wang, Y.J., 2018. Reconstructing  
1174 South China in Phanerozoic and Precambrian supercontinents. *Earth-Science Reviews*,  
1175 186: 173-194.

1176 Cenko, B., Braun, I. and Bröcker, M., 2004. Evolution of the continental crust in the Kerala  
1177 Khondalite Belt, southernmost India: evidence from Nd isotope mapping, U–Pb and Rb–  
1178 Sr geochronology. *Precambrian Research*, 134: 275-292.

1179 Chen, X., Zhou, Y. and Shields, G.A., 2022. Progress towards an improved Precambrian  
1180 seawater  $^{87}\text{Sr}/^{86}\text{Sr}$  curve. *Earth-Science Reviews*, 224: 103869.

1181 Clark, C., Collins, A.S., Santosh, M., Taylor, R. and Wade, B.P., 2009. The P-T-t architecture of  
1182 a Gondwanan suture: REE, U-Pb and Ti-in-zircon thermometric constraints from the  
1183 Palghat Cauvery shear system, South India. *Precambrian Research*, 174(1-2): 129-144.

1184 Clark, C., Collins, A.S., Taylor, R.J.M. and Hand, M., 2020. Isotopic systematics of zircon  
1185 indicate an African affinity for the rocks of southernmost India. *Scientific Reports*.

1186 Clark, C., Healy, D., Johnson, T., Collins, A.S., Taylor, R.J., Santosh, M. and Timms, N.E.,  
1187 2015. Hot orogens and supercontinent amalgamation: A Gondwanan example from  
1188 southern India. *Gondwana Research*, 28(4): 1310-1328.

1189 Cohen, K., Harper, D., Gibbard, P. and Car, N., 2025. The ICS international chronostratigraphic  
1190 chart this decade. *Episodes* 48.

1191 Collins, A., 2006. The tectonic evolution of Madagascar: Its place in the East African orogen.  
1192 *Gondwana Research*, 3(4): 549-552.

1193 Collins, A. and Pisarevsky, S., 2005. Amalgamating eastern Gondwana: The evolution of the  
1194 Circum-Indian Orogens. *Earth-Science Reviews*, 71(3-4): 229-270.

1195 Collins, A. and Windley, B., 2002. The tectonic evolution of central and northern Madagascar  
1196 and its place in the final assembly of Gondwana. *Journal of Geology*, 110(3): 325-339.

1197 Collins, A.S., Ali, J.R. and Razakamanana, T., 2022a. An Introduction to the Geology of  
1198 Madagascar. In: S.M. Goodman (Editor), *The new natural history of Madagascar*.  
1199 Princeton University Press, Princeton, pp. 45-51.

1200 Collins, A.S., Blades, M.L. and Merdith, A.S., 2021a. The Arabian–Nubian Shield Within the  
1201 Neoproterozoic Plate Tectonic Circuit. In: Z. Hamimi, A.-R. Fowler, J.-P. Liégeois, A.  
1202 Collins, M.G. Abdelsalam and M. Abd Ei-Wahed (Editors), *The Geology of the Arabian-*  
1203 *Nubian Shield*. Springer International Publishing, Cham, pp. 195-202.

1204 Collins, A.S., Blades, M.L., Merdith, A.S. and Foden, J.D., 2021b. Closure of the Proterozoic  
1205 Mozambique Ocean was instigated by a late Tonian plate reorganization event.  
1206 *Communications Earth & Environment*, 2(1).

1207 Collins, A.S., Cameron, F., Blades, M.L., Hasterok, D., Simpson, A., Gilbert, S., Clark, C. and  
1208 Makin, S., 2022b. Size is everything: reconstructing the East African Orogen—a

1209 Gondwanan supermountain—as a critical step to modelling the Neoproterozoic earth  
1210 system, Goldschmidt, Hawaii.

1211 Collins, A.S., Clark, C. and Plavsa, D., 2014. Peninsular India in Gondwana: The tectonothermal  
1212 evolution of the Southern Granulite Terrain and its Gondwanan counterparts. *Gondwana*  
1213 *Research*, 25(1): 190-203.

1214 Collins, A.S., Clark, C., Sajeev, K., Santosh, M., Kelsey, D.E. and Hand, M., 2007. Passage  
1215 through India: the Mozambique Ocean suture, high-pressure granulites and the Palghat-  
1216 Cauvery shear zone system. *Terra Nova*, 19(2): 141-147.

1217 Collins, A.S., Kinny, P.D. and Razakamanana, T., 2012. Depositional age, provenance and  
1218 metamorphic age of metasedimentary rocks from southern Madagascar. *Gondwana*  
1219 *Research*, 21(2-3): 353-361.

1220 Collins, A.S., Kröner, A., Fitzsimons, I.C.W. and Razakamanana, T., 2003. Detrital Footprint of  
1221 the Mozambique Ocean: U/Pb SHRIMP and Pb Evaporation Zircon Geochronology of  
1222 Metasedimentary Gneisses in Eastern Madagascar. *Tectonophysics*, 375: 77-99.

1223 Collins, A.S., Redaa, A., Vecoli, M. and Alwaheed, A., 2024. Age of the basement to the  
1224 Arabian petroleum system: U-Pb zircon/apatite and in-situ Rb-Sr LA-ICP-MS/MS dates  
1225 from beneath central and east Saudi Arabia, AAPG ICE 2024, Muscat.

1226 Coolen, J.J.M.M., Priem, H.N.A., Verdurmen, E.A.T. and Verschure, R.H., 1982. Possible  
1227 zircon U-Pb evidence for Pan-African granulite-facies metamorphism in the Mozambique  
1228 belt of southern Tanzania. *Precambrian Research*, 17: 31-40.

1229 Costa, R.L., Schmitt, R.S., Collins, A.S., Armistead, S.E., Gomes, I.V., Archibald, D.B. and  
1230 Razakamanana, T., 2021. Tectonic evolution of an Early Cryogenian late-magmatic basin  
1231 in central Madagascar. *Journal of African Earth Sciences*, 179: 104205.

1232 Cox, G.M., Foden, J. and Collins, A.S., 2019. Late Neoproterozoic adakitic magmatism of the  
1233 eastern Arabian Nubian Shield. *Geoscience Frontiers*, 10(6): 1981-1992.

1234 Cox, G.M., Halverson, G.P., Stevenson, R.K., Vokaty, M., Poirier, A., Kunzmann, M., Li, Z.X.,  
1235 Denyszyn, S.W., Strauss, J.V. and Macdonald, F.A., 2016a. Continental flood basalt  
1236 weathering as a trigger for Neoproterozoic Snowball Earth. *Earth and Planetary Science*  
1237 *Letters*, 446: 89-99.

1238 Cox, G.M., Jarrett, A., Edwards, D., Crockford, P.W., Halverson, G.P., Collins, A.S., Poirier, A.  
1239 and Li, Z.X., 2016b. Basin redox and primary productivity within the Mesoproterozoic  
1240 Roper Seaway. *Chemical Geology*, 440: 101-114.

1241 Cox, G.M., Lewis, C.J., Collins, A.S., Halverson, G.P., Jourdan, F., Foden, J., Nettle, D. and  
1242 Kattan, F., 2012. Ediacaran terrane accretion within the Arabian-Nubian Shield.  
1243 *Gondwana Research*, 21(2-3): 341-352.

1244 Cox, R., Armstrong, R.A. and Ashwal, L.D., 1998. Sedimentology, geochronology and  
1245 provenance of the Proterozoic Itremo Group, central Madagascar, and implications for  
1246 pre-Gondwana palaeogeography. *Journal of the Geological Society, London*, 155: 1009-  
1247 1024.

1248 Cox, R., Coleman, D., Chokel, C., DeOreo, S., Wooden, J., Collins, A., De Waele, B. and  
1249 Kroner, A., 2004. Proterozoic tectonostratigraphy and paleogeography of central  
1250 Madagascar derived from detrital zircon U-Pb age populations. *Journal of Geology*,  
1251 112(4): 379-399.

1252 Cozzi, A., Rea, G. and Craig, J., 2012. From global geology to hydrocarbon exploration:  
1253 Ediacaran-Early Cambrian petroleum plays of India, Pakistan and Oman. *Geological*  
1254 *Society, London, Special Publications*, 366(1): 131-162.

- 1255 Cutten, H., Johnson, S.P. and De Waele, B., 2006. Protolith Ages and Timing of Metasomatism  
1256 Related to the Formation of Whiteschists at Mautia Hill, Tanzania: Implications for the  
1257 Assembly of Gondwana. *Journal of Geology*, 114: 683–698.
- 1258 Dal Piaz, G.V., Ibrahim, H.A., Martin, S., Piccardo, G.B., Rigatti, G. and Venturelli, G., 1993.  
1259 Pan-African Metabasalts from the Maydh Area, North-Eastern Somalia. In: E. Abbate,  
1260 M. Sagri and F.P. Sassi (Editors), *Geology and Mineral Resources of Somalia and*  
1261 *Surrounding Regions*. Instituto Agronomico per l'Oltremare, Firenze, pp. 41-58.
- 1262 Dalziel, I.W.D., 1997. Neoproterozoic-Paleozoic geography and tectonics: Review, hypothesis,  
1263 environmental speculation. *Geological Society of America Bulletin*, 109(1): 16-42.
- 1264 Davies, R.G. and Crawford, A.R., 1971. Petrography and Age of Rocks of Bulland-Hill, Kirana-  
1265 Hills, Sarghoda District, West Pakistan. *Geological Magazine*, 108(3): 235-&.
- 1266 de Wall, H., Regelous, A., Tomaschek, F., Bestmann, M., Hahn, G. and Sharma, K.K., 2022.  
1267 Tonian evolution of an active continental margin - a model for Neoproterozoic NW  
1268 India-SE Pakistan–E Oman linkage. *Precambrian Research*, 381: 106822.
- 1269 de Wit, M.J. and Linol, B., 2015. Precambrian Basement of the Congo Basin and Its Flanking  
1270 Terrains. In: M.J. de Wit, F. Guillocheau and M.C.J. de Wit (Editors), *Geology and*  
1271 *Resource Potential of the Congo Basin*. Regional Geology Reviews. Springer-Verlag,  
1272 Berlin Heidelberg, pp. 19--37.
- 1273 Deb, M., Thorpe, R.I., Krstic, D., Corfu, F. and Davis, D.W., 2001. Zircon U-Pb and galena Pb  
1274 isotope evidence for an approximate 1.0 Ga terrane constituting the western margin of the  
1275 Aravalli-Delhi orogenic belt, northwestern India. *Precambrian Research*, 108: 195-213.
- 1276 Derry, L.A. and France-Lanord, C., 1996. Neogene Himalayan weathering history and  
1277 river<sup>87</sup>Sr<sup>86</sup>Sr: impact on the marine Sr record. *Earth and Planetary Science Letters*,  
1278 142(1): 59-74.
- 1279 Djerosse, F., Berger, J., Vanderhaeghe, O., Isseini, M., Ganne, J. and Zeh, A., 2020.  
1280 Neoproterozoic magmatic evolution of the southern Ouaddaï Massif (Chad) Open  
1281 Access. *Bulletin de la Societe Geologique de France*, 191: 34.
- 1282 Doebrich, J.L., Al-Jehani, A.M., Siddiqui, A.A., Hayes, T.S., Wooden, J.L. and Johnson, P.R.,  
1283 2007. Geology and metalogeny of the Ar Rayn terrane, eastern Arabian shield: Evolution  
1284 of a Neoproterozoic continental-margin arc during assembly of Gondwana within the  
1285 East African orogen. *Precambrian Research*, 158: 17-50.
- 1286 Domeier, M., 2016. A plate tectonic scenario for the Iapetus and Rheic oceans. *Gondwana*  
1287 *Research*, 36: 275-295.
- 1288 Domeier, M. and Torsvik, T.H., 2014. Plate tectonics in the late Paleozoic. *Geoscience Frontiers*,  
1289 5(3): 303-350.
- 1290 Drury, S.A. and De Souza, C.R., 1998. Neoproterozoic terrane assemblages in Eritrea: review  
1291 and prospects. *Journal of African Earth Sciences*, 27(3-4): 331-348.
- 1292 Eguíluz, L., Puelles, P., Tarrío, A. and Abalos, B., 2024. The Neoproterozoic Mozambique Belt  
1293 in the Gol Mountains (N Tanzania): Structural Analysis of Amphibolite and Granulite-  
1294 Facies Nappe Tectonites From a Crustal Orogenic Channel. *Tectonics*, 43(11).
- 1295 Elburg, M.A., Andersen, T., Jacobs, J., Laufer, A., Ruppel, A., Krohne, N. and Damaske, D.,  
1296 2016. One Hundred Fifty Million Years of Intrusive Activity in the Sor Rondane  
1297 Mountains (East Antarctica): Implications for Gondwana Assembly. *Journal of Geology*,  
1298 124(1): 1-26.

1299 Eyal, M., Be'eri-Shlevin, Y., Eyal, Y., Whitehouse, M.J. and Litvinovsky, B., 2014. Three  
1300 successive Proterozoic island arcs in the Northern Arabian-Nubian Shield: Evidence from  
1301 SIMS U-Pb dating of zircon. *Gondwana Research*, 25(1): 338-357.

1302 Fergusson, C.L., Nutman, A.P., Mohajjel, M. and Bennett, V.C., 2016. The Sanandaj-Sirjan  
1303 Zone in the Neo-Tethyan suture, western Iran: Zircon U-Pb evidence of late Palaeozoic  
1304 rifting of northern Gondwana and mid-Jurassic orogenesis. *Gondwana Research*, 40: 43-  
1305 57.

1306 Flowerdew, M.J., Whitehouse, M.J. and Stoesser, D.B., 2013. The Nabitah fault zone, Saudi  
1307 Arabia: A Pan-African suture separating juvenile oceanic arcs. *Precambrian Research*,  
1308 239: 95-105.

1309 Frisch, W. and Pohl, W., 1986. Petrochemistry of some mafic and ultramafic rocks from the  
1310 Mozambique Belt, SE Kenya. *Mitteilungen der Oesterreichischen Geologischen*  
1311 *Gesellschaft*, 78: 97-114.

1312 Fritz, H., Abdelsalam, M., Ali, K.A., Bingen, B., Collins, A.S., Fowler, A.R., Ghebreab, W.,  
1313 Hauzenberger, C.A., Johnson, P., Kusky, T., Macey, P., Muhongo, S., Stern, R.J. and  
1314 Viola, G., 2013. Orogen styles in the East Africa Orogens: A review of the  
1315 Neoproterozoic to Cambrian Tectonic Evolution. *Journal of African Earth Sciences*, 86:  
1316 65-106.

1317 Fritz, H. and Hauzenberger, C., 2021. The Southern Part of the Arabian–Nubian Shield in Kenya  
1318 and Tanzania. In: Z. Hamimi, A.-R. Fowler, J.-P. Liégeois, A. Collins, M.G. Abdelsalam  
1319 and M. Abd Ei-Wahed (Editors), *The Geology of the Arabian-Nubian Shield*. Springer  
1320 International Publishing, Cham, pp. 63-80.

1321 Gessner, K., Collins, A., Ring, U. and Gungor, T., 2004. Structural and thermal history of poly-  
1322 orogenic basement: U-Pb geochronology of granitoid rocks in the southern Menderes  
1323 Massif, Western Turkey. *Journal of the Geological Society*, 161: 93-101.

1324 Ghosh, J.G., de Wit, M.J. and Zartman, R.E., 2004. Age and tectonic evolution of  
1325 Neoproterozoic ductile shear zones in the Southern Granulite Terrain of India, with  
1326 implications for Gondwana studies. *Tectonics*, 23(TC3006): doi:10.1029/2002TC001444.

1327 Glen, R.A. and Meffre, S., 2009. Styles of Cenozoic collisions in the western and southwestern  
1328 Pacific and their applications to Palaeozoic collisions in the Tasmanides of eastern  
1329 Australia. *Tectonophysics*, 479(1-2): 130-149.

1330 Godderis, Y., Donnadieu, Y., Carretier, S., Aretz, M., Dera, G., Macouin, M. and Regard, V.,  
1331 2017. Onset and ending of the late Palaeozoic ice age triggered by tectonically paced  
1332 rock weathering. *Nature Geoscience*, 10(5): 382-+.

1333 Gomes, I.V., Schmitt, R.S., Rosenbaum, G., Armistead, S.E. and Mussili, J.V.S., 2025. The  
1334 triple orogenic junction of central Gondwana. *International Geology Review*, 67(12):  
1335 1533-1560.

1336 Gómez-Pérez, I. and Morton, A., 2025. Neoproterozoic–early Paleozoic tectonic evolution of  
1337 Oman revisited: implications for the consolidation of Gondwana. *Geological Society*,  
1338 London, Special Publications, 550(1): SP550-2024-36.

1339 Gómez-Pérez, I., Morton, A., Rawahi, H.A. and Frei, D., 2024. Oman as a fragment of Ediacaran  
1340 eastern Gondwana. *Geology*, 52(6): 473-478.

1341 Goscombe, B., Foster, D.A., Gray, D. and Wade, B., 2020. Assembly of central Gondwana along  
1342 the Zambezi Belt: Metamorphic response and basement reactivation during the Kuunga  
1343 Orogeny. *Gondwana Research*, 80: 410-465.

- 1344 Goscombe, B., Foster, D.A., Gray, D., Wade, B., Marsellos, A. and Titus, J., 2017. Deformation  
1345 correlations, stress field switches and evolution of an orogenic intersection: The Pan-  
1346 African Kaoko-Damara orogenic junction, Namibia. *Geoscience Frontiers*, 8(6): 1187-  
1347 1232.
- 1348 Gregory, L.C., Meert, J.G., Bingen, B., Pandit, M.K. and Torsvik, T.H., 2009. Paleomagnetism  
1349 and geochronology of the Malani Igneous Suite, Northwest India: Implications for the  
1350 configuration of Rodinia and the assembly of Gondwana. *Precambrian Research*, 170(1-  
1351 2): 13-26.
- 1352 Guru Rajesh, K. and Chetty, T.R.K., 2006. Structure and tectonics of the Achancovil Shear  
1353 Zone, southern India. *Gondwana Research*, 10: 86-98.
- 1354 Halverson, G.P., Hurtgen, M., Porter, S.M. and Collins, A.S., 2010. Neoproterozoic-Cambrian  
1355 Biogeochemical Evolution. In: C. Gaucher, A. Sial, G.P. Halverson and H. Frimmel  
1356 (Editors), *Events at the Precambrian-Cambrian boundary: a focus on southwestern*  
1357 *Gondwana*. Elsevier, *Developments in Precambrian Geology*, Amsterdam.
- 1358 Hamimi, Z., Eldosouky, A.M., Hagag, W. and Kamh, S.Z., 2023. Large-scale geological  
1359 structures of the Egyptian Nubian Shield. *Scientific Reports*, 13(1): 1923.
- 1360 Handke, M.J., Tucker, R.D. and Hamilton, M.A., 1997. Early Neoproterozoic (800-790 Ma)  
1361 intrusive igneous rocks in central Madagascar; geochemistry and petrogenesis. *Abstracts*  
1362 *with Programs*, 29: 468.
- 1363 Harms, U., Darbyshire, D.P.F., Denkler, T., Hengst, M. and Schandelmeier, H., 1994. Evolution  
1364 of the Neoproterozoic Delgo Suture Zone and crustal growth in northern Sudan:  
1365 geochemical and radiogenic isotope constrains. *Geologische Rundschau*, 83: 591–603.
- 1366 Hasterok, D. and Chapman, D.S., 2007. Continental thermal isostasy: 1. Methods and sensitivity.  
1367 *Journal of Geophysical Research: Solid Earth*, 112(B6).
- 1368 Hauenberger, C.A., Sommer, H., Fritz, H., Bauernhofer, A., Kröner, A., Hoinkes, G.,  
1369 Wallbrecher, E. and Thöni, M., 2007. SHRIMP U-Pb zircon and Sm-Nd garnet ages from  
1370 the granulite facies basement of SE-Kenya: evidence for Neoproterozoic polycyclic  
1371 assembly of the Mozambique Belt. *Journal of the Geological Society, London*, 164: 189-  
1372 201.
- 1373 Honarmand, M., Xiao, W.J., Nabatian, G., Blades, M.L., dos Santos, M.C., Collins, A.S. and Ao,  
1374 S.J., 2018. Zircon U-Pb-Hf isotopes, bulk-rock geochemistry and Sr-Nd-Pb isotopes from  
1375 late Neoproterozoic basement in the Mahneshan area, NW Iran: Implications for  
1376 Ediacaran active continental margin along the northern Gondwana and constraints on the  
1377 late Oligocene crustal anatexis. *Gondwana Research*, 57: 48-76.
- 1378 Jacobs, J., Elburg, M., Laufer, A., Kleinhanns, I.C., Henjes-Kunst, F., Estrada, S., Ruppel, A.S.,  
1379 Damaske, D., Montero, P. and Bea, F., 2015. Two distinct Late Mesoproterozoic/Early  
1380 Neoproterozoic basement provinces in central/eastern Dronning Maud Land, East  
1381 Antarctica: The missing link, 15-21 degrees E. *Precambrian Research*, 265: 249-272.
- 1382 Jamshidi-Badr, M., Collins, A.S., Masoudi, F., Cox, G. and Mohajel, M., 2013. The U-Pb age,  
1383 geochemistry and tectonic significance of granitoids in The Soursat complex, Northwest  
1384 Iran. *Turkish Journal of Earth Sciences*, 22: 1-31.
- 1385 John, T., Schenk, V., Mezger, K. and Tembo, F., 2004. Timing and PT evolution of whiteschist  
1386 metamorphism in the Lufilian Arc-Zambezi Belt Orogen (Zambia): Implications for the  
1387 assembly of Gondwana. *Journal of Geology*, 112(1): 71-90.
- 1388 Johnson, P.R., Andresen, A., Collins, A.S., Fowler, A.R., Fritz, H., Ghebreab, W., Kusky, T. and  
1389 Stern, R.J., 2011. Late Cryogenian-Ediacaran history of the Arabian-Nubian Shield: A

1390 review of depositional, plutonic, structural, and tectonic events in the closing stages of  
1391 the northern East African Orogen. *Journal of African Earth Sciences*, 61(3): 167-232.

1392 Johnson, P.R. and Stewart, I.C.F., 1995. Magnetically inferred basement structure in central  
1393 Saudi Arabia. *Tectonophysics*, 245: 37-52.

1394 Johnson, P.R. and Woldehaimanot, B., 2003. Development of the Arabian-Nubian Shield:  
1395 perspectives on accretion and deformation in the northern East African Orogen and the  
1396 assembly of Gondwana. In: M. Yoshida, B.F. Windley and S. Dasgupta (Editors),  
1397 Proterozoic East Gondwana: Supercontinent Assembly and Breakup. Geological Society,  
1398 London, Special Publication 206, pp. 289-325.

1399 Johnson, S.P., Cutten, H.N.C., Muhongo, S. and De Waele, B., 2003. Neoproterozoic magmatism  
1400 and metamorphism of the western granulites in the central domain of the Mozambique  
1401 belt, Tanzania: U-Pb SHRIMP geochronology and PT estimates. *Tectonophysics*, 375:  
1402 125-145.

1403 Johnson, S.P., De Waele, B. and Liyungu, K.A., 2006. U-Pb sensitive high-resolution ion  
1404 microprobe (SHRIMP) zircon geochronology of granitoid rocks in eastern Zambia:  
1405 Terrane subdivision of the Mesoproterozoic Southern Irumide Belt - art. no. TC6004.  
1406 *Tectonics*, 25(6): C6004-C6004.

1407 Johnson, T.E., Clark, C., Taylor, R.J.M., Santosh, M. and Collins, A.S., 2015. Prograde and  
1408 retrograde growth of monazite in migmatites: An example from the Nagercoil Block,  
1409 southern India. *Geoscience Frontiers*, 6(3): 373-387.

1410 Jöns, N. and Schenk, V., 2008. Relics of the Mozambique Ocean in the central East African  
1411 Orogen: evidence from the Vohibory Block of southern Madagascar. *Journal of*  
1412 *Metamorphic Geology*, 26: 17-28.

1413 Jöns, N., Schenk, V., John, T. and Razakamanana, T., 2005. Relics of the Mozambique Ocean:  
1414 geochemistry of the Vohibory Block (Madagascar). In: M.T.D. Wingate and S.A.  
1415 Pisarevsky (Editors), Supercontinents and Earth Evolution. Geological Society of  
1416 Australia, Abstracts, No. 81, Fremantle, pp. 133.

1417 Just, J., Schulz, B., de Wall, H., Jourdan, F. and Pandit, M.K., 2011. Monazite CHIME/EPMA  
1418 dating of Erinpura granitoid deformation: Implications for Neoproterozoic tectono-  
1419 thermal evolution of NW India. *Gondwana Research*, 19(2): 402-412.

1420 Kashghari, W., Collins, A.S., Nehlig, P., Abu El-Enen, M.M., Macey, P.H., Jacobs, J., Passchier,  
1421 C., Kattan, F.H., Whitehouse, M., Bakhsh, R., Al Garni, S.M., Elkomi, M.B., Johnson,  
1422 P.R., Stern, R.J., Harbi, F.M.H., Rimi, N.N. and Qubsani, A.N., 2025. Critical Review of  
1423 the Stratigraphy Framework of the Arabian Shield: Current Understanding and  
1424 Knowledge Gaps. Saudi Geological Survey Special Publication Report.

1425 Kazmin, V., 1975. Explanation of the geological map of Ethiopia. Memoir of the Ethiopian  
1426 Institute of Geological Survey.

1427 Kitano, I., Osanai, Y., Nakano, N., Adachi, T. and Fitzsimons, I.C.W., 2018. Detrital zircon and  
1428 igneous protolith ages of high-grade metamorphic rocks in the Highland and Wann  
1429 Complexes, Sri Lanka: Their geochronological correlation with southern India and East  
1430 Antarctica. *Journal of Asian Earth Sciences*, 156: 122-144.

1431 Koralay, O.E., Dora, O.O., Chen, F., Satir, M. and Candan, O., 2004. Geochemistry and  
1432 geochronology of orthogneisses in the derbent (Alasehir) area, eastern part of the  
1433 Odemis-Kiraz submassif, Menderes Massif: Pan-African magmatic activity. *Turkish*  
1434 *Journal of Earth Sciences*, 13(1): 37-61.

- 1435 Kröner, A., Hegner, E., Collins, A., Windley, B., Brewer, T., Razakamanana, T. and Pidgeon, R.,  
1436 2000. Age and magmatic history of the Antananarivo Block, central Madagascar, as  
1437 derived from zircon geochronology and Nd isotopic systematics. *American Journal of*  
1438 *Science*, 300(4): 251-288.
- 1439 Kröner, A. and Jaekel, P., 1994. Zircon ages from rocks of the Wannii complex, Sri Lanka.  
1440 *Journal of the Geological Society of Sri Lanka*, 5: 41-57.
- 1441 Kröner, A., Kovach, V., Belousova, E., Hegner, E., Armstrong, R., Dolgoplova, A., Seltmann,  
1442 R., Alexeiev, D.V., Hoffmann, J.E., Wong, J., Sun, M., Cai, K., Wang, T., Tong, Y.,  
1443 Wilde, S.A., Degtyarev, K.E. and Rytisk, E., 2014. Reassessment of continental growth  
1444 during the accretionary history of the Central Asian Orogenic Belt. *Gondwana Research*,  
1445 25(1): 103-125.
- 1446 Kröner, A., Muhongo, S., Hegner, E. and Wingate, M.T.D., 2003. Single-zircon geochronology  
1447 and Nd isotopic systematics of Proterozoic high-grade rocks from the Mozambique belt  
1448 of southern Tanzania (Masasi area): implications for Gondwana assembly. *Journal of the*  
1449 *Geological Society, London*, 160: 745-757.
- 1450 Kröner, A., Sacchi, R., Jaekel, P. and Costa, M., 1997. Kibaran magmatism and Pan-African  
1451 granulite metamorphism in northern Mozambique: single zircon ages and regional  
1452 implications. *Journal of African Earth Sciences*, 25(3): 467-484.
- 1453 Kröner, A., Santosh, M. and Wong, J., 2012. Zircon ages and Hf isotopic systematics reveal  
1454 vestiges of Mesoproterozoic to Archaean crust within the late Neoproterozoic–Cambrian  
1455 high-grade terrain of southernmost India. *Gondwana Research*, 21: 876-886.
- 1456 Kröner, A. and Sassi, F.P., 1996. Evolution of the northern Somali basement: new constraints  
1457 from zircon ages. *Journal of African Earth Sciences*, 22: 1-15.
- 1458 Kumar, T.V., Rao, Y.J.B., Plavsa, D., Collins, A.S., Tomson, J.K., Gopal, B.V. and Babu,  
1459 E.V.S.S.K., 2017. Zircon U-Pb ages and Hf isotopic systematics of charnockite gneisses  
1460 from the Ediacaran-Cambrian high-grade metamorphic terranes, southern India:  
1461 Constraints on crust formation, recycling, and Gondwana correlations. *Geological*  
1462 *Society of America Bulletin*, 129(5-6): 625-648.
- 1463 Kusky, T.M. and Matsah, M.I., 2003. Neoproterozoic dextral faulting on the Najd Fault System,  
1464 Saudi Arabia, preceded sinistral faulting and escape tectonics related to closure of the  
1465 Mozambique Ocean. In: M. Yoshida, B. Windley and S. Dasgupta (Editors), *Proterozoic*  
1466 *East Gondwana: Supercontinent Assembly and Breakup*. Geological Society, London,  
1467 Special Publication 206, pp. 327-361.
- 1468 Küster, D., Utke, A., Leupolt, L., Lenoir, J.L. and Haider, A., 1990. Pan-African granitoid  
1469 magmatism in northeastern and southern Somalia. *Berliner Geowissenschaftliche*  
1470 *Abhandlungen*, 120: 519-536.
- 1471 Lenoir, J.-L., Küster, D., Liégeois, J.-P., Utke, A., Haider, A. and Matheis, G., 1994. Origin and  
1472 regional significance of late Precambrian and early Palaeozoic granitoids in the Pan-  
1473 African belt of Somalia. *Geologische Rundschau*, 83: 624-641.
- 1474 Li, Z.-X., Liu, Y. and Ernst, R., 2023. A dynamic 2000—540 Ma Earth history: From cratonic  
1475 amalgamation to the age of supercontinent cycle. *Earth-Science Reviews*, 238: 104336.
- 1476 Li, Z.X., Bogdanova, S.V., Collins, A.S., Davidson, A., De Waele, B., Ernst, R.E., Fitzsimons,  
1477 I.C.W., Fuck, R.A., Gladkochub, D.P., Jacobs, J., Karlstrom, K.E., Lu, S., Natapov, L.M.,  
1478 Pease, V., Pisarevsky, S.A., Thrane, K. and Vernikovskiy, V., 2008. Assembly,  
1479 configuration, and break-up history of Rodinia: A synthesis. *Precambrian Research*,  
1480 160(1-2): 179-210.

1481 Lom, N., Şengör, A.M.C., Zabcı, C., Sunal, G. and Öner, T., 2024. The Saharides: Reassessing  
1482 the Nature and History of the Pan-African Events in North Africa and the Arabian Shield.  
1483 In: Z. Hamimi, M.C. Chabou, E. Errami, A.-R. Fowler, N. Fello, A. Masrouhi and R.  
1484 Leprêtre (Editors), *The Geology of North Africa. Regional Geology Reviews*. Springer.  
1485 Loosveld, R., Bell, A. and Terken, J., 1996. The tectonic evolution of Interior Oman. *Georabia*,  
1486 1: 28-51.

1487 Maboko, M.A.H., 2000. Nd and Sr isotopic investigation of the Archean–Proterozoic boundary  
1488 in north eastern Tanzania: constraints on the nature of Neoproterozoic tectonism in the  
1489 Mozambique Belt. *Precambrian Research*, 102(1): 87-98.

1490 Mänttari, I., Kigereigu, F., Huhma, H., Kock, G.S., Koistinen, T., Kuosmanen, E.T., Lahaye, Y.,  
1491 Lehtonen, M.I., Mäkitie, H., Manninen, T., O'Brien, H., Saalman, K., Virransalo, P. and  
1492 Westerhof, A., 2011. New Precambrian rock ages from Uganda. Abstracts Volume, 23rd  
1493 Colloquium of African Geology, 8-14 January 2011, Johannesburg, South Africa.

1494 McIntyre, A., 2023. High-grade metamorphism in Turkana, Kenya: implications for the  
1495 evolution of the East African Orogen, The University of Adelaide, Adelaide, 94 pp.

1496 McWilliams, M.O., 1981. Palaeomagnetism and Precambrian tectonic evolution of Gondwana.  
1497 In: A. Kröner (Editor), *Precambrian Plate Tectonics*. Elsevier, Amsterdam, pp. 649-687.

1498 Meert, J.G., Pandit, M.K. and Kamenov, G.D., 2013. Further geochronological and  
1499 paleomagnetic constraints on Malani (and pre-Malani) magmatism in NW India.  
1500 *Tectonophysics*, 608: 1254-1267.

1501 Meert, J.G. and Van der Voo, R., 1997. The assembly of Gondwana 800-550 Ma. *Journal of*  
1502 *Geodynamics*, 23: 223-236.

1503 Merdith, A.S., Collins, A.S., Williams, S.E., Pisarevsky, S., Foden, J.D., Archibald, D.B.,  
1504 Blades, M.L., Alessio, B.L., Armistead, S., Plavsa, D., Clark, C. and Muller, R.D., 2017a.  
1505 A full-plate global reconstruction of the Neoproterozoic. *Gondwana Research*, 50: 84-  
1506 134.

1507 Merdith, A.S., Williams, S.E., Collins, A.S., Tetley, M.G., Mulder, J.A., Blades, M.L., Young,  
1508 A., Armistead, S.E., Cannon, J., Zahirovic, S. and Müller, R.D., 2021. Extending full-  
1509 plate tectonic models into deep time: Linking the Neoproterozoic and the Phanerozoic.  
1510 *Earth-Science Reviews*, 214: 103477.

1511 Merdith, A.S., Williams, S.E., Muller, R.D. and Collins, A.S., 2017b. Kinematic constraints on  
1512 the Rodinia to Gondwana transition. *Precambrian Research*, 299: 132-150.

1513 Merdith, A.S., Wright, N.M., Williams, S., Hunter, S.J., J., L., Blades, M.L., F., B., Supadee, K.,  
1514 Gurung, K., Xu, Z., Hasterok, D., Collins, A.S. and Mills, B.J.W., Submitted. Process-  
1515 based simulation of palaeogeography and topography over the 1 last billion years. *Earth-*  
1516 *Science Reviews*.

1517 Meyer, S.E., Passchier, C., Abu-Alam, T. and Stüwe, K., 2014. A strike-slip core complex from  
1518 the Najd fault system, Arabian shield. *Terra Nova*, 26(5): 387-394.

1519 Mills, B.J.W., le Hir, G., Merdith, A., Gurung, K., Bowyer, F.T., Krause, A.J., Sanchez-  
1520 Baracaldo, P., Hunter, S.J. and Zhang, Y., 2025. Exploring Neoproterozoic climate and  
1521 biogeochemical evolution in the SCION model. *Global and Planetary Change*, 249:  
1522 104791.

1523 Mohammed, M.A.I., 2017. The geology of the western Nuba Mountains region, South Kordofan  
1524 State, Sudan, with special emphasis on the low-grade Neoproterozoic meta-volcano-  
1525 sedimentary sequence, University of Pretoria, 200 pp.

- 1526 Mole, D.R., Barnes, S.J., Taylor, R.J.M., Kinny, P.D. and Fritz, H., 2018. A relic of the  
1527 Mozambique Ocean in south-east Tanzania. *Precambrian Research*, 305: 386-426.
- 1528 Möller, A., Mezger, K. and Schenk, V., 2000. U-Pb dating of metamorphic minerals: Pan-  
1529 African metamorphism and prolonged slow cooling of high pressure granulites in  
1530 Tanzania, East Africa. *Precambrian Research*, 104: 123-146.
- 1531 Moore, J.M., 1979. Tectonics of the Najd Transcurrent Fault System, Saudi Arabia. *Journal of*  
1532 *the Geological Society*, 136(4): 441-452.
- 1533 Muhongo, S., 1994. Neoproterozoic Collision Tectonics In the Mozambique Belt Of East- Africa  
1534 - Evidence From the Uluguru Mountains, Tanzania. *Journal Of African Earth Sciences*,  
1535 19: 153-168.
- 1536 Muhongo, S., Kröner, A. and Nemchin, A.A., 2001. Single zircon evaporation and SHRIMP  
1537 ages for granulite-facies rocks in the Mozambique belt of Tanzania. *Journal of Geology*,  
1538 109: 171-189.
- 1539 Nance, R.D., Worsley, T.R. and Moody, J.B., 1988. The Supercontinent Cycle. *Scientific*  
1540 *American*, 259(1): 72-79.
- 1541 Nettle, D., Halverson, G.P., Cox, G.M., Collins, A.S., Schmitz, M., Gehling, J., Johnson, P.R.  
1542 and Kadi, K., 2014. A middle-late Ediacaran volcano-sedimentary record from the  
1543 eastern Arabian-Nubian shield. *Terra Nova*, 26(2): 120-129.
- 1544 Neves, S.P., Bruguier, O., Vauchez, A., Bosch, D., da Silva, J.M.R. and Mariano, G., 2006.  
1545 Timing of crust formation, deposition of supracrustal sequences, and Transamazonian  
1546 and Brasiliano metamorphism in the East Pernambuco belt (Borborema Province, NE  
1547 Brazil): Implications for western Gondwana assembly. *Precambrian Research*, 149(3-4):  
1548 197-216.
- 1549 Nutman, A.P., Mohajjel, M., Bennett, V.C. and Fergusson, C.L., 2014. Gondwanan Eoarchean-  
1550 Neoproterozoic ancient crustal material in Iran and Turkey: zircon U-Pb-Hf isotopic  
1551 evidence. *Canadian Journal of Earth Sciences*, 51(3): 272-285.
- 1552 Pandit, M.K., Carter, L.M., Ashwal, L.D., Tucker, R.D., Torsvik, T.H., Jamtveit, B. and  
1553 Bhushan, S.K., 2003. Age, petrogenesis and significance of 1 Ga granitoids and related  
1554 rocks from the Sendra area, Aravalli Craton, NW India. *Journal of Asian Earth Sciences*,  
1555 22: 363-381.
- 1556 Park, Y., Swanson-Hysell, N.L., MacLennan, S.A., Maloof, A.C., Gebreslassie, M., Tremblay,  
1557 M.M., Schoene, B., Alene, M., Anttila, E.S.C., Tesema, T. and Haileab, B., 2019. The  
1558 lead-up to the Sturtian Snowball Earth: Neoproterozoic chemostratigraphy time-  
1559 calibrated by the Tambien Group of Ethiopia. *GSA Bulletin*, 132(5-6): 1119-1149.
- 1560 Plavsa, D., Collins, A.S., Foden, J.D. and Clark, C., 2015. The evolution of a Gondwanan  
1561 collisional orogen: A structural and geochronological appraisal from the Southern  
1562 Granulite Terrane, South India. *Tectonics*, 34(5): 820-857.
- 1563 Plavsa, D., Collins, A.S., Foden, J.F., Kropinski, L., Santosh, M., Chetty, T.R.K. and Clark, C.,  
1564 2012. Delineating crustal domains in Peninsular India: Age and chemistry of  
1565 orthopyroxene-bearing felsic gneisses in the Madurai Block. *Precambrian Research*, 198:  
1566 77-93.
- 1567 Plavsa, D., Collins, A.S., Payne, J.L., Foden, J.D., Clark, C. and Santosh, M., 2014. Detrital  
1568 Zircons in Basement Metasedimentary Protoliths Unveil the Origins of Southern India.  
1569 *Geological Society of America, Bulletin*, in press.
- 1570 Plunder, A., Blein, O., Isseini, M., Al-Gadam, I.O., Chevillard, M., Djedouboum, E., Lach, P.,  
1571 Lahfid, A., Melleton, J., Rouzeau, O. and Vic, G., 2026. A window on the amalgamation

1572 of Western Gondwana: Geological history of the Ouaddaï massif (E. Chad). *Precambrian*  
1573 *Research*, 434: 108000.

1574 Rajendra Prasad, B., Kesava Rao, G., Mall, D.M., Koteswara Rao, P., Raju, S., Reddy, M.S.,  
1575 Rao, G.S.P., Sridher, V. and Prasad, A.S.S.S.R.S., 2007. Tectonic implications of seismic  
1576 reflectivity pattern observed over the Precambrian Southern Granulite Terrain, India.  
1577 *Precambrian Research*, 53: 1-10.

1578 Ramakrishnan, M., 1993. Tectonic Evolution of the Granulite Terrains of Southern India.  
1579 *Continental Crust of South India*(25): 35-44.

1580 Ramezani, J. and Tucker, R.D., 2003. The Saghand region, central Iran: U-Pb geochronology,  
1581 petrogenesis and implications for Gondwana tectonics. *American Journal Of Science*,  
1582 303: 622-665.

1583 Rantakokko, N.E., Whitehouse, M.J., Pease, V. and Windley, B.F., 2014. Neoproterozoic  
1584 evolution of the eastern Arabian basement based on a refined geochronology of the  
1585 Marbat region, Sultanate of Oman. *Tectonic Evolution of the Oman Mountains*, 392:  
1586 107-127.

1587 Raza, M., Ahmad, A.H.M., Khan, M.S. and Khan, F., 2012. Geochemistry and detrital modes of  
1588 Proterozoic sedimentary rocks, Bayana Basin, north Delhi fold belt: implications for  
1589 provenance and source-area weathering. *International Geology Review*, 54(1): 111-129.

1590 Reddy, S., Collins, A. and Mruma, A., 2003. Complex high-strain deformation in the Usagaran  
1591 Orogen, Tanzania: structural setting of Palaeoproterozoic eclogites. *Tectonophysics*,  
1592 375(1-4): 101-123.

1593 Reeves, C.V., de Wit, M.J. and Sahu, B.K., 2004. Tight reassembly of Gondwana exposes  
1594 Phanerozoic shears in Africa as global tectonic players. *Gondwana Research*, 7: 7-20.

1595 Ries, A.C., Vearncombe, J.R., Price, R.C. and Shackleton, R.M., 1992. Geochronology and  
1596 Geochemistry of the Rocks Associated with a Late Proterozoic Ophiolite in West Pokot,  
1597 Nw Kenya. *Journal of African Earth Sciences*, 14(1): 25-36.

1598 Robinson, F.A., Foden, J.D. and Collins, A.S., 2015a. Geochemical and isotopic constraints on  
1599 island arc, synorogenic, post-orogenic and anorogenic granitoids in the Arabian Shield,  
1600 Saudi Arabia. *Lithos*, 220: 97-115.

1601 Robinson, F.A., Foden, J.D. and Collins, A.S., 2015b. Zircon Geochemical and  
1602 Geochronological Constraints on Contaminated and Enriched Mantle Sources beneath the  
1603 Arabian Shield, Saudi Arabia. *Journal of Geology*, 123(5): 463-489.

1604 Robinson, F.A., Foden, J.D., Collins, A.S. and Payne, J.L., 2014. Arabian Shield magmatic  
1605 cycles and their relationship with Gondwana assembly: Insights from zircon U-Pb and Hf  
1606 isotopes. *Earth and Planetary Science Letters*, 408: 207-225.

1607 Rosenbaum, G., 2018. The Tasmanides: Phanerozoic Tectonic Evolution of Eastern Australia.  
1608 *Annual Review of Earth and Planetary Sciences*, Vol 46, 46: 291-325.

1609 Rossetti, F., Nozaem, R., Lucci, F., Vignaroli, G., Gerdes, A., Nasrabadi, M. and Theye, T.,  
1610 2015. Tectonic setting and geochronology of the Cadomian (Ediacaran-Cambrian)  
1611 magmatism in Central Iran, Kuh-e-Sarhangi region (NW Lut Block). *Journal of Asian*  
1612 *Earth Sciences*, 102: 24-44.

1613 Sacchi, R., Cadoppi, P. and Costa, M., 2000. Pan-African reactivation of the Lurio segment of  
1614 the Kibaran Belt system: a reappraisal from recent age determinations in northern  
1615 Mozambique. *Journal of African Earth Sciences*, 30(3): 629-639.

1616 Santosh, M., Maruyama, S. and Sato, K., 2009. Anatomy of a Cambrian suture in Gondwana:  
1617 Pacific type orogeny in southern India? *Gondwana Research*, 16: 321-341.

- 1618 Santosh, M., Tagawa, M., Taguchi, S. and Yoshikura, S., 2003. The Nagercoil Granulite Block,  
1619 southern India: petrology, fluid inclusions and exhumation history. *Journal of Asian*  
1620 *Earth Sciences*, 22: 131-155.
- 1621 Santosh, M., Tagawa, M., Yokoyama, K. and Collins, A.S., 2006. U-Pb electron probe  
1622 geochronology of the Nagercoil granulites, southern India: Implications for Gondwana  
1623 amalgamation. *Journal of Asian Earth Sciences*, 28(1): 63-80.
- 1624 Sassi, F.P. and Visonà, D., 1993. Relics of Granulitic Mineral Assemblages in the Northern  
1625 Somali Basement. In: E. Abbate, M. Sagri and F.P. Sassi (Editors), *Geology and Mineral*  
1626 *Resources of Somalia and Surrounding Regions*. Istituto Agronomico per l'Oltremare,  
1627 Firenze, pp. 83-90.
- 1628 Sassi, F.P., Visonà, D., Ferrara, G., Gatto, G.O., Ibrahim, H.A., Said, A.A. and Tonarini, S.,  
1629 1993. The Crystalline Basement of Northern Somalia: Lithostratigraphy and the  
1630 Sequence of Events. In: E. Abbate, M. Sagri and F.P. Sassi (Editors), *Geology and*  
1631 *Mineral Resources of Somalia and Surrounding Regions*. Istituto Agronomico per  
1632 l'Oltremare, Firenze, pp. 3-40.
- 1633 Schandelmeier, H., Rahman, E.A., Wipfler, E., Küster, D., Utke, A. and Matheis, G., 1994. Late  
1634 Proterozoic magmatism in the Nakasib suture, Red Sea Hills, Sudan. *Journal of the*  
1635 *Geological Society*, 151(3): 485-497.
- 1636 Schmitt, R.d.S., Fragoso, R.d.A. and Collins, A.S., 2018. Suturing Gondwana in the Cambrian:  
1637 The Orogenic Events of the Final Amalgamation. In: S. Siegesmund, M.A.S. Basei, P.  
1638 Oyhantçabal and S. Oriolo (Editors), *Geology of Southwest Gondwana*. Springer  
1639 International Publishing, Cham, pp. 411-432.
- 1640 Schoff, W.H., 1912. *The Periplus of the Erythræan sea; travel and trade in the Indian Ocean*.  
1641 Longmans, Green, and Co., New York, 323 p. pp.
- 1642 Schreurs, G., Giese, J., Berger, A. and Gnos, E., 2010. A new perspective on the significance of  
1643 the Ranotsara shear zone in Madagascar. *International Journal of Earth Sciences*, 99(8):  
1644 1827-1847.
- 1645 Scotese, C.R., 2021. An Atlas of Phanerozoic Paleogeographic Maps: The Seas Come In and the  
1646 Seas Go Out. *Annual Review Earth and Planetary Sciences*, 49: 679-728.
- 1647 Şengör, A.M.C., Lom, N., Zabcı, C., Sunal, G. and Öner, T., 2020. Reconstructing orogens  
1648 without biostratigraphy: The Saharides and continental growth during the final assembly  
1649 of Gondwana-Land. *Proceedings of the National Academy of Sciences*, 117(51): 32278-  
1650 32284.
- 1651 Shackleton, R.M., 1996. The final collision between East and West Gondwana; where is it?  
1652 *Journal of African Earth Sciences*, 23: 271-287.
- 1653 Shakoor, M.A., Yang, X.Y., Deng, J.H. and Hakro, A.A.A.D., 2019. Early Neoproterozoic  
1654 evolution of Southeast Pakistan: evidence from geochemistry, geochronology, and  
1655 isotopic composition of the Nagarparkar Igneous Complex. *International Geology*  
1656 *Review*, 61(11): 1391-1408.
- 1657 Shellnutt, J.G., Pham, N.H.T., Denyszyn, S.W., Yeh, M.-W. and Lee, T.-Y., 2017. Timing of  
1658 collisional and post-collisional Pan-African Orogeny silicic magmatism in south-central  
1659 Chad. *Precambrian Research*, 301: 113-123.
- 1660 Shellnutt, J.G., Yeh, M.-W. and Lee, T.-Y., 2026. Is the continental crust of North-Central Africa  
1661 a metacraton or a shield terrane?: the view from Chad. *Journal of African Earth Sciences*,  
1662 233: 105875.

1663 Shen, C., Schmitz, M., Johnson, P., Davies, J.H.F.L. and Halverson, G.P., 2022. U-Pb  
1664 geochronology and cyclostratigraphy of the middle Ediacaran upper Jibalah Group,  
1665 eastern Arabian Shield. *Precambrian Research*, 375.

1666 Shields, G.A., 2007. A normalised seawater strontium isotope curve: possible implications for  
1667 Neoproterozoic-Cambrian weathering rates and the further oxygenation of the Earth.  
1668 *eEarth*, 2(2): 35-42.

1669 Sommer, H., Kröner, A., Hauenberger and Muhongo, S., 2003. Metamorphic petrology and  
1670 zircon geochronology of high-grade rocks from the central Mozambique belt of Tanzania.  
1671 *Journal of Metamorphic Geology*, 21: 915-934.

1672 Squire, R.J., Campbell, I.H., Allen, C.M. and Wilson, C.J.L., 2006. Did the Transgondwanan  
1673 Supermountain trigger the explosive radiation of animals on Earth? *Earth and Planetary  
1674 Science Letters*, 250(1-2): 116-133.

1675 Stampfli, G.M., 2005. Plate tectonics of the Apulia-Adria Microcontinents. In: I.R. Finetti  
1676 (Editor), *CROP PROJECT: Deep Seismic Exploration of the Central Mediterranean and  
1677 Italy*. Elsevier, Amsterdam.

1678 Stern, R.J., 1994. Arc Assembly and continental collision in the Neoproterozoic East African  
1679 orogeny - implications for the consolidation of Gondwana. *Annual Review of Earth and  
1680 Planetary Sciences*, 22: 319-351.

1681 Stern, R.J. and Johnson, P., 2010. Continental lithosphere of the Arabian Plate: A geologic,  
1682 petrologic, and geophysical synthesis. *Earth-Science Reviews*, 101(1-2): 29-67.

1683 Stoesser, D.B. and Frost, C.D., 2006. Nd, Pb, Sr, and O isotopic characterization of Saudi Arabian  
1684 shield terranes. *Chemical Geology*, 226(3-4): 163-188.

1685 Swanson-Hysell, N.L., Maloof, A.C., Condon, D.J., Jenkin, G.R.T., Alene, M., Tremblay, M.M.,  
1686 Tesema, T., Rooney, A.D. and Haileab, B., 2015. Stratigraphy and geochronology of the  
1687 Tambien Group, Ethiopia: Evidence for globally synchronous carbon isotope change in  
1688 the Neoproterozoic. *Geology*, 43(4): 323-326.

1689 Swanson-Hysell, N.L., Zhang, Y.M., Macdonald, F.A., Koran, I., Tasistro-Hart, A.R. and Jay,  
1690 A.F., 2025. Oman was on the northern margin of a wide late Tonian Mozambique Ocean.  
1691 *Geology*, 53(11).

1692 Tamblyn, R., Hand, M., Simpson, A., Gilbert, S., Wade, B. and Glorie, S., 2022. laser ablation  
1693 Lu-Hf geochronology of garnet across the Western Gneiss Region: campaign-style dating  
1694 of metamorphism. *Journal of the Geological Society*, 179(4).

1695 Tang, M., Chu, X., Hao, J. and Shen, B., 2021. Orogenic quiescence in Earth's middle age.  
1696 *Science*, 371(6530): 728-731.

1697 Taylor, R.J.M., Clark, C., Fitzsimons, I.C.W., Santosh, M., Hand, M., Evans, N. and McDonald,  
1698 B., 2014. Post-peak, fluid-mediated modification of granulite facies zircon and monazite  
1699 in the Trivandrum Block, southern India. *Contributions to Mineralogy and Petrology*,  
1700 168(2).

1701 Teklay, M., Kröner, A., Mezger, K. and Oberhänsli, R., 1998. Geochemistry, Pb-Pb single zircon  
1702 ages and Nd-Sr isotope composition of Precambrian rocks from southern and eastern  
1703 Ethiopia: implications for crustal evolution in East Africa. *Journal of African Earth  
1704 Sciences*, 26: 207-227.

1705 Tenczer, V., Hauenberger, C., Fritz, H., Hoinkes, G., Muhongo, S. and Klotzli, U., 2013.  
1706 Crustal age domains and metamorphic reworking of the deep crust in Northern-Central  
1707 Tanzania: a U/Pb zircon and monazite age study. *Mineralogy and Petrology*, 107(5): 679-  
1708 707.

- 1709 Thomas, R.J., De Waele, B., Schofield, D.I., Goodenough, K.M., Horstwood, M., Tucker, R.D.,  
1710 Bauer, W., Annells, R., Howard, K., Walsh, G., Rabarimanana, M., Rafahatelo, J.-M.,  
1711 Ralison, A.V. and Randriamananjara, T., 2009. Geological evolution of the  
1712 Neoproterozoic Bemarivo Belt, northern Madagascar. *Precambrian Research*, 172: 279-  
1713 300.
- 1714 Thomas, R.J., Ellison, R.A., Goodenough, K.M., Roberts, N.M.W. and Allen, P.A., 2015. Salt  
1715 domes of the UAE and Oman: Probing eastern Arabia. *Precambrian Research*, 256: 1-16.
- 1716 Torsvik, T.H., Ashwal, L.D., Tucker, R.D. and Eide, E.A.P.R., 2001. Geochronology and  
1717 paleomagnetism of the Seychelles microcontinent: The India link. *Precambrian Research*,  
1718 110: 47-59.
- 1719 Torsvik, T.H. and Cocks, L.R.M., 2013. New global palaeogeographical reconstructions for the  
1720 Early Palaeozoic and their generation. *Early Palaeozoic Biogeography and*  
1721 *Palaeogeography*, 38: 5-24.
- 1722 Toteu, S.F., de Wit, M., Penaye, J., Drost, K., Tait, J.A., Bouyo, M.H., Van Schmus, W.R.,  
1723 Jelsma, H., Moloto-A-Kenguemba, G.R., da Silva, A.F., Lerouge, C. and Doucouré, M.,  
1724 2022. Geochronology and correlations in the Central African Fold Belt along the northern  
1725 edge of the Congo Craton: New insights from U-Pb dating of zircons from Cameroon,  
1726 Central African Republic, and south-western Chad. *Gondwana Research*, 107: 296-324.
- 1727 Tucker, R.D., Amelin, Y., Belcher, R.W., Delor, C., Goncalves, P., Rabarimanana, M.H. and  
1728 Ralison, A.V., 2011. Neoproterozoic extension in the Greater Dharwar Craton: a  
1729 reevaluation of the "Betsimisaraka suture" in Madagascar. *Canadian Journal Of Earth*  
1730 *Sciences*, 48: 389-417.
- 1731 Tucker, R.D., Ashwal, L.D., Handke, M.J., Hamilton, M.A., Le Grange, M. and Rabeloson,  
1732 R.A., 1999. U-Pb geochronology and isotope geochemistry of the Archean and  
1733 Proterozoic rocks of north-central Madagascar. *Journal of Geology*, 107: 135-153.
- 1734 Tucker, R.D., Ashwal, L.D. and Torsvik, T.H., 2001. U-Pb geochronology of Seychelles  
1735 granitoids: a Neoproterozoic continental arc fragment. *Earth and Planetary Science*  
1736 *Letters*, 187: 27-38.
- 1737 Tucker, R.D., Roig, J.Y., Moine, B., Delor, C. and Peters, S.G., 2014. A geological synthesis of  
1738 the Precambrian shield in Madagascar. *Journal of African Earth Sciences*, 94: 9-30.
- 1739 Ustaomer, P.A., Ustaomer, T., Collins, A.S. and Robertson, A.H.F., 2009. Cadomian (Ediacaran-  
1740 Cambrian) arc magmatism in the Bitlis Massif, SE Turkey: Magmatism along the  
1741 developing northern margin of Gondwana. *Tectonophysics*, 473(1-2): 99-112.
- 1742 Vail, J.R., 1985. Pan-African (late Precambrian) tectonic terrains and the reconstruction of the  
1743 Arabian-Nubian Shield. *Geology*, 13: 839-842.
- 1744 Van Lente, B., Ashwal, L.D., Pandit, M.K., Bowring, S.A. and Torsvik, T.H., 2009.  
1745 Neoproterozoic hydrothermally altered basaltic rocks from Rajasthan, northwest India:  
1746 Implications for late Precambrian tectonic evolution of the Aravalli Craton. *Precambrian*  
1747 *Research*, 170(3-4): 202-222.
- 1748 Vearncombe, J.R., 1983. A Proposed Continental-Margin in the Precambrian of Western Kenya.  
1749 *Geologische Rundschau*, 72(2): 663-670.
- 1750 Veizer, J., Ala, D., Azmy, K., Bruckschen, P., Buhl, D., Bruhn, F., Carden, G.A.F., Diener, A.,  
1751 Ebner, S., Godderis, Y., Jasper, T., Korte, C., Pawellek, F., Podlaha, O.G. and Strauss,  
1752 H., 1999.  $^{87}\text{Sr}/^{86}\text{Sr}$ ,  $\delta^{13}\text{C}$  and  $\delta^{18}\text{O}$  evolution of Phanerozoic seawater. *Chemical*  
1753 *Geology*, 161(1): 59-88.

- 1754 Vincent, V.I., Torremans, K., Subarkah, D., Gilbert, S.E., Farkaš, J., Collins, A.S., Stacey, J.,  
1755 Doran, A.L., Jones, S. and Hitzman, M.W., 2026. In situ Rb–Sr geochronology records  
1756 multiple fluid pulses in Neoproterozoic sequences from the Lubambe-Mingomba Cu  
1757 deposits in the Zambian Copperbelt. *Precambrian Research*, 437: 108059.
- 1758 Viola, G., Henderson, I.H.C., Bingen, B., Thomas, R.J., Smethurst, M.A. and de Azavedo, S.,  
1759 2008. Growth and collapse of a deeply eroded orogen: Insights from structural,  
1760 geophysical, and geochronological constraints on the Pan-African evolution of NE  
1761 Mozambique. *Tectonics*, 27(5).
- 1762 Vollstaedt, H., Eisenhauer, A., Wallmann, K., Bohm, F., Fietzke, J., Liebetrau, V., Krabbenhoft,  
1763 A., Farkas, J., Tomasovych, A., Raddatz, J. and Veizer, J., 2014. The Phanerozoic delta  
1764 Sr-88/86 record of seawater: New constraints on past changes in oceanic carbonate  
1765 fluxes. *Geochimica Et Cosmochimica Acta*, 128: 249-265.
- 1766 von Raumer, J.F., Stampfli, G.A. and Bussy, F., 2003. Gondwana-derived microcontinents - the  
1767 constituents of the Variscan and Alpine collisional orogens. *Tectonophysics*, 365(1-4): 7-  
1768 22.
- 1769 Wang, W., Cawood, P.A., Zhou, M.F., Pandit, M.K., Xia, X.P. and Zhao, J.H., 2017. Low-delta  
1770 O-18 Rhyolites From the Malani Igneous Suite: A Positive Test for South China and NW  
1771 India Linkage in Rodinia. *Geophysical Research Letters*, 44(20): 10298-10305.
- 1772 Wegener, A., 1912. Die Entstehung der Kontinente. *Geologische Rundschau*, 3(4): 276-292.
- 1773 Westerhof, A.B.P., Härmä, P., Isabirye, E., Katto, E., Koistinen, T., Kuosmanen, E., Lehto, T.,  
1774 Lehtonen, M.I., Mäkitie, H., Manninen, T., Mänttari, I., Pekkala, Y., Pokki, J., Saalman,  
1775 K. and Virransalo, P., 2014. Geology and Geodynamic Development of Uganda with  
1776 Explanation of the 1:1,000,000 Scale Geological Map. Geological Survey of Finland,  
1777 Special Paper, Geological Survey of Finland.
- 1778 Whitehouse, M.J., Flowerdew, M.J., Petersson, A., Al-Khribash, S. and Stoeser, D.B., 2025. The  
1779 Amlah terrane, Yemen – a missing link in the Neoproterozoic tectonic collage of the  
1780 Arabian Shield. *Geological Society, London, Special Publications*, 550(1): SP550-2024-  
1781 128.
- 1782 Whitehouse, M.J., Flowerdew, M.J., Stoeser, D.B. and Stacey, J.S., 2023. The Khida terrane -  
1783 Isotopic evidence for Paleoproterozoic to Neoproterozoic basement in the eastern Arabian  
1784 Shield. *Precambrian Research*, 399.
- 1785 Whitehouse, M.J., Pease, V. and Al-Khribash, S., 2016. Neoproterozoic crustal growth at the  
1786 margin of the East Gondwana continent - age and isotopic constraints from the  
1787 easternmost inliers of Oman. *International Geology Review*, 58(16): 2046-2064.
- 1788 Whitehouse, M.J., Windley, B.F., Ba-Bttat, M.A.O., Fanning, C.M. and Rex, D.C., 1998. Crustal  
1789 evolution and terrane correlation in the eastern Arabian Shield, Yemen: geochronological  
1790 constraints. *Journal of the Geological Society*, 155: 281-295.
- 1791 Whitehouse, M.J., Windley, B.F., Stoeser, D.B., Al-Khribash, S., Ba-Bttat, M.A.O. and Haider,  
1792 A., 2001. Precambrian basement character of Yemen and correlations with Saudi Arabia  
1793 and Somalia. *Precambrian Research*, 105(2-4): 357-369.
- 1794 Windley, B.F., Whitehouse, M.J. and BaBttat, M.A.O., 1996. Early precambrian gneiss terranes  
1795 and Pan-African island arcs in Yemen: Crustal accretion of the eastern Arabian Shield.  
1796 *Geology*, 24(2): 131-134.
- 1797 Xiao, W.J., Song, D.F., Windley, B.F., Li, J.L., Han, C.M., Wan, B., Zhang, J., Ao, S.J. and  
1798 Zhang, Z.Y., 2020. Accretionary processes and metallogenesis of the Central Asian

1799 Orogenic Belt: Advances and perspectives. *Science China-Earth Sciences*, 63(3): 329-  
1800 361.

1801 Yang, B., Collins, A.S., Cox, G.M., Jarrett, A.J.M., Denyszyn, S., Blades, M.L., Farkaš, J. and  
1802 Glorie, S., 2020. Using Mesoproterozoic Sedimentary Geochemistry to Reconstruct  
1803 Basin Tectonic Geography and Link Organic Carbon Productivity to Nutrient Flux from a  
1804 Northern Australian Large Igneous Province. *Basin Research*, 32.

1805 Yeshanew, F.G., Pease, V., Abdelsalam, M.G. and Whitehouse, M.J., 2017. Zircon U-Pb ages,  
1806 delta O-18 and whole-rock Nd isotopic compositions of the Dire Dawa Precambrian  
1807 basement, eastern Ethiopia: implications for the assembly of Gondwana. *Journal of the  
1808 Geological Society*, 174(1): 142-156.

1809 Yeshanew, F.G., Pease, V., Whitehouse, M.J. and Al-Khirbash, S., 2015. Zircon U-Pb  
1810 geochronology and Nd isotope systematics of the Abas terrane, Yemen: Implications for  
1811 Neoproterozoic crust reworking events. *Precambrian Research*, 267: 106-120.

1812 Zhang, W., Pease, V., Whitehouse, M.J., El-Sankary, M.M. and Shalaby, M.H., 2019. Pre-  
1813 Neoproterozoic basement evolution of southwestern Egypt. *International Geology  
1814 Review*, 61(15): 1909-1926.

1815 Zhou, J., Farahbakhsh, E., Williams, S., Li, X., Liu, Y., Li, S. and Müller, R.D., 2025. Machine  
1816 Learning and Big Data Mining Reveal Earth's Deep Time Crustal Thickness and Tectonic  
1817 Evolution: A New Chemical Mohometry Approach. *Journal of Geophysical Research:  
1818 Solid Earth*, 130(5): e2024JB030404.

1819 Zhu, Z., Campbell, I.H., Allen, C.M., Brocks, J.J. and Chen, B., 2022. The temporal distribution  
1820 of Earth's supermountains and their potential link to the rise of atmospheric oxygen and  
1821 biological evolution. *Earth and Planetary Science Letters*, 580: 117391.

1822 Zoleikhaei, Y., Cawood, P.A. and Mulder, J.A., 2025. Non-arc setting for "Cadomian"  
1823 magmatism in Iran and Anatolia. *Geoscience Frontiers*, 16(2): 101995.

1824 Zuza, A. V., Levy, D. A., and Mulligan, S. R., 2022, Geologic field evidence for non-lithostatic  
1825 overpressure recorded in the North American Cordillera hinterland, northeast Nevada,  
1826 *Geosci. Frontiers*, 13, 101099, doi: 10.1016/j.gsf.2020.10.006.